

A NOVEL POWER FLOW METHOD FOR
LONG TERM FREQUENCY STABILITY ANALYSIS

A Thesis

by

WENJIN YAN

Submitted to the Office of Graduate Studies of
Texas A&M University
in partial fulfillment of the requirements for the degree of

MASTER OF SCIENCE

Approved by:

Chair of Committee,
Committee Members,

Head of Department,

Garng M. Huang
Chanan Singh
Shankar P. Bhattacharyya
Guergana Petrova
Chanan Singh

May 2013

Major Subject: Electrical Engineering

Copyright 2013 Wenjin Yan

ABSTRACT

This thesis presents a novel approach for a power system to find a practical power flow solution when all the generators in the system have hit their real power output limits, such as some generator units shutting down or load outages. The approach assumes the frequency of the system is unable to be kept at the rated value (usually 60 or 50 Hz) and accordingly, the generator real power outputs are affected by the system frequency deviation.

The modification aims to include the system frequency deviation as a new state variable in the power flow so that the power system can be described in a more precise way when the generation limits are hit and the whole system is not operated under the normal condition. A new mathematical formulation for power flow is given by modified the conventional power flow mismatch equation and Jacobian matrix.

The Newton – Raphson method is particularly chose to be modified because Newton – Raphson method is most widely used and it is a fast convergent and accurate method. The Jacobian matrix will be augmented by adding a column and a row.

Matlab is used as a programming tool to implement the Power Flow for Long Term Frequency Stability (PFLTFS) method for a simple 4-bus system and the IEEE 118-bus system. And PSS/E Dynamic simulation is used to verify the steady state solution from PFLTFS is reasonable. The PSS/E Dynamic Simulation plots are used to analyze the long term frequency response.

The PFLTFS method provides a technique for solving an abnormal state system power flow. From the results we can conclude that the PFLTFS method is reasonable for solving power flow of a real power unbalanced system.

ACKNOWLEDGEMENTS

I am heartily thankful to my committee chair, Dr. Huang, whose encouragement, guidance and support from the initial to the final level enabled me to develop an understanding of the subject.

I would like to thank my committee members, Dr. Singh, Dr. Bhattacharyya, and Dr. Petrova, for their guidance and support throughout the course of this research.

Thanks also go to my friends and colleagues and the department faculty and staff for making my time at Texas A&M University a great experience.

In addition, I offer my regards and blessings to all of those who supported me in any respect during the completion of the project.

Finally, thanks to my father, mother and my eldest aunt for their encouragement.

TABLE OF CONTENTS

| | Page |
|--|------|
| ABSTRACT | ii |
| ACKNOWLEDGEMENTS | iii |
| TABLE OF CONTENTS | iv |
| LIST OF FIGURES | vi |
| LIST OF TABLES | viii |
| CHAPTER I INTRODUCTION AND LITERATURE REVIEW | 1 |
| 1.1 Background | 1 |
| 1.2 Motivation | 3 |
| 1.3 Objectives..... | 4 |
| 1.4 Literature Review..... | 4 |
| CHAPTER II POWER FLOW METHOD..... | 6 |
| 2.1 Power Flow Equation..... | 6 |
| 2.2 Newton - Raphson Method | 12 |
| 2.3 NR Method in Power Flow Analysis | 15 |
| CHAPTER III THEORETICAL FRAMEWORK..... | 20 |
| 3.1 Frequency Stability | 20 |
| 3.2 Frequency Control..... | 21 |
| 3.3 A Novel Power Flow Method | 26 |
| CHAPTER IV PSS/E ENVIRONMENT AND DYNAMIC MODEL | 44 |
| 4.1 PSS/E Environment..... | 44 |
| 4.2 Dynamic Model..... | 46 |
| 4.3 Frequency Response..... | 54 |
| CHAPTER V STUDY CASE MODELING AND SIMULATION..... | 56 |
| 5.1 A 4-bus System Case Study | 56 |
| 5.2 IEEE 118-bus System Scenarios | 74 |
| CHAPTER VI DISCUSSION AND CONCLUSION | 91 |

| | |
|---|----|
| 6.1 Possible Causes of the Frequency Difference | 91 |
| 6.2 Conclusion..... | 92 |
| REFERENCES | 95 |

LIST OF FIGURES

| | Page |
|--|------|
| Figure 1 A 4-bus System | 7 |
| Figure 2 Droop Characteristic | 23 |
| Figure 3 Turbine-Governor Generator System..... | 24 |
| Figure 4 Secondary Loop Control | 25 |
| Figure 5 Flow Chart of PFLTFS Method | 43 |
| Figure 6 Generator Model Data Sheet..... | 46 |
| Figure 7 TGOV1 Model [18]..... | 47 |
| Figure 8 TGOV1 Dynamic Data | 48 |
| Figure 9 TGOV5 Model [20]..... | 48 |
| Figure 10 TGOV5 Dynamic Data | 49 |
| Figure 11 SEXS Exciter Model [22] | 51 |
| Figure 12 SEXS Dynamic Data..... | 51 |
| Figure 13 IEEEET2 Model [24]..... | 52 |
| Figure 14 IEEEET2 Dynamic Data | 52 |
| Figure 15 IEEEEST Dynamic Data | 53 |
| Figure 16 A simple 4-bus System..... | 57 |
| Figure 17 4-bus System PF Converted Save Case..... | 61 |
| Figure 18 4-bus System Dynamic Data File..... | 61 |
| Figure 19 Long-term System Frequency Response..... | 63 |
| Figure 20 System Frequency Response in First 120s..... | 64 |
| Figure 21 The Long-term System Frequency Response..... | 65 |

| | |
|--|----|
| Figure 22 Voltage at Bus-1..... | 67 |
| Figure 23 Voltage at Bus-2 and Bus-3 | 67 |
| Figure 24 Voltage at Bus-1 in First 120s..... | 68 |
| Figure 25 Load at Bus-2 and Bus-3..... | 69 |
| Figure 26 The Generator Output Power and Mechanical Power at Bus-1 | 70 |
| Figure 27 P_{elec} and P_{mech} at Bus-1 in First 120s..... | 71 |
| Figure 28 IEEE 118-bus System | 75 |
| Figure 29 IEEE 118-bus System PF Save Case..... | 77 |
| Figure 30 IEEE 118-bus Dynamic Data..... | 77 |
| Figure 31 Long-term System Frequency Response..... | 79 |
| Figure 32 Frequency Response from 20s-60s | 80 |
| Figure 33 P_{mech} and P_{elec} at Bus-80 | 81 |
| Figure 34 Voltage and Load at Bus-80..... | 82 |
| Figure 35 Frequency Responses in Scenario 1 and 2 | 83 |
| Figure 36 Frequency Responses in Scenario 1 and 2 from 20s~60s | 84 |
| Figure 37 Mechanical Power at Bus-80 in Scenario 1 and 2..... | 85 |

LIST OF TABLES

| | Page |
|--|------|
| Table 1 State Variables..... | 31 |
| Table 2 4-bus System Power Flow Solution | 60 |
| Table 3 4-bus System Dynamic Simulation Solution..... | 62 |
| Table 4 PF Solution with a Constant Impedance Load | 66 |
| Table 5 PF Solution with a Mixed Load..... | 74 |
| Table 6 Results Compared Scenario 1..... | 78 |
| Table 7 Results Compared in Scenario 2..... | 83 |
| Table 8 Results Compared in Scenario 3..... | 86 |
| Table 9 Results Compared in Scenario 4..... | 87 |
| Table 10 Frequency Results (30% Output Tripped)..... | 88 |
| Table 11 Frequency Results (40% Output Tripped)..... | 89 |
| Table 12 Frequency Results (50% Output Tripped)..... | 89 |
| Table 13 Frequency Results (40% Output Tripped, K=18)..... | 90 |
| Table 14 Frequency Results (40% Output Tripped, K=8)..... | 90 |

CHAPTER I

INTRODUCTION AND LITERATURE REVIEW

1.1 Background

As the rapidly increasing load demands, the stress on power system is increasing. It cannot be denied that frequency stability is becoming another major problem for power system because of both environmental and economic reasons.

For environmental concerns, renewable energy such as wind power and solar power are considered to be the most clean and economic energy sources. It was estimated that by the end of 2009 the total installed world wind energy capacity would reach 150 GW, indicating a 25% annual average growth rate in wind energy capacity [1]. The existing system is a system with much higher wind penetrations than ever before. In the coming decade off-shore wind power is also expected to expand rapidly. For solar energy power, photovoltaic production growth has averaged 40% per year since 2000 and installed capacity reached 39.8 GW at the end of 2010 [2].

However, one of the primary disadvantages to wind power and solar power is they are intermittent energy sources. The variability of wind makes wind generations are much likely to be shutting down because it is weather dependent, and sometimes it is unpredictable. To solar energy, it is only available at daytime and is also subject to intermittence due to drifting clouds. These uncertainties bring an unprecedented challenge to power system stability, especially frequency stability. When the wind is not available as predicted, many generations will hit the limits and thus the frequency will start getting lower and thus the long term stability occurs. During this period, we also are concerned about the power flows during frequency deviations.

On the other hand, due to the economic and environmental concerns, the existing system will be more utilized since it is becoming difficult to build new power plants and transmission

lines [3]. Economic and environmental requirements force the utilities to maximize the use of the system [4]. That is to say, the existing system is operating at a state that is very close to the limits of the elements in the system. Under this situation, the possibility of generators outage or tie-line tripping will be higher than before. This is why long term frequency stability becomes a critical issue.

In the past, the frequency is usually considered as a static variable and the worldwide major concerns are about voltage stability. For most systems, the system frequency is kept at a rated value (usually at 60 or 50 Hz). However, the frequency is a good indicator of power system long term stability.

Generally, frequency instability is the result of generators shutting down or load outages. The frequency deviation is usually caused by the imbalance between generations and loads. The result of generators shutting down or load outages is a long-term distortion in the power balance. The imbalance is initially covered from kinetic energy of rotating rotors of turbines, generators and motors, as a result, the frequency in the system will change [5].

In addition, in power system Newton - Raphson method is widely used to find power flow solutions for a system. It is fast converged and accurate. However, the conventional Newton - Raphson method is operated under 2 assumptions. One is the generations are considered plenty to balance the load all the time. The slack bus can always cover the mismatch part of the system. Accordingly, the frequency is considered to be steady at 60 Hz. In fact, the generation of slack bus has its maximum value and frequency is a variable depends on how much rotation energy is needed to be extracted to balance the load. In order to analyze the power flow under the circumstance, this thesis provides a method to incorporate the long term frequency deviation into power flow and then analyze the long term frequency response after units tripping in a system.

1.2 Motivation

In this thesis, a novel method is presented for the power system to find a power flow solution including the system frequency. It deals with the problem when some or all the generators in the system have hit their real power output limits, which may occur after wind power generation is gone unexpectedly for example. This thesis focuses on how a system frequency responds at the steady state and the corresponding line flows as generations hit the limits

Under this study, all the generators' real power outputs have their limits and the system frequency deviation is related to the generator real power output due to the generator's droop characteristics. Then the novel power flow method can include the system frequency deviation as a new state variable of the system. The Newton – Raphson method is particularly chose to be modified because Newton – Raphson method is most widely used and it is a fast convergent and accurate method to find the power flow solution for power system.

In Newton – Raphson method, the conventional power flow mismatch equation is modified by adding a new state variable, the system frequency deviation. The relation between the frequency deviation and the generator mechanical power is considered. And the Jacobian matrix is also modified by adding a column whose elements are the power derivative of frequency deviation. However, an extra variable needs an extra equation to have a solution. Details will be presented later.

The software Matlab is used as a programming tool to implement the Power Flow Long Term Frequency Stability (PFLTFS) method. A simple 4 – bus system and IEEE 118 – bus system are used to demonstrate our approach. PSS/E Dynamic simulation function is used to verify the static state solution from PFLTFS is reasonable. The system frequency response is

also analyzed and divided into four stages using the frequency figures from PSS/E dynamic simulation.

With this Power Flow for Long Term Frequency Stability method, a steady state power flow solution is obtained that includes the system frequency for a power system either operated under a normal condition or under an abnormal condition.

1.3 Objectives

The overall objectives of this work are:

To develop and validate a power flow method which incorporates the system frequency deviation as a new state variable.

To apply the novel power flow method to both small and big system examples and use PSS/E to verify the power flow results.

To analyze the long term frequency response of a system which have its generators reach their limits and operate in an abnormal state.

1.4 Literature Review

In this section, some of the relevant literature in the research areas of frequency stability and power flow method are reviewed. There are main differences between the proposed method and the prior works.

A paper [6] addresses a power flow method with FACTS devices for a system which is not under a normal state. The paper considers the load model to be a time varying piecewise static load with a daily load curve.

Although this paper develops an efficient load flow technique for ill-condition radial distribution their model does not address the problem of the frequency deviation and thus unable to deal with long term stability with frequency deviation.

A paper [7] develops a fast algorithm considering the effect of frequency deviation on loads and generator outputs for static state for a Dispatcher Training Simulator (DTS). The paper deals with a non-symmetric Jacobian matrix resulting from the presence of frequency deviation and it is fast decoupled which helps to meet the real time requirements of Dispatcher Training Simulator.

Although this paper also includes the frequency into the power flow, it does not address the issue with the slack bus in power flow analysis. With an extra variable $\Delta\omega$, we need an extra equation. In addition, the generations in the paper are within the limits and the systems are operating in a normal state. Thus there will be no need to incorporate the frequency into the power flow because the frequency deviation is within a very narrow range and the steady state system frequency can be considered stable. The author did not realize that frequency is only an issue when the generation and loads are extremely imbalanced and thus frequency responds and starts a long-term frequency stability situation. Using power flow to catch frequency deviation is unrealistic and dynamic simulation is needed to catch the frequency deviation. Power flow analysis is only valid for steady state analysis.

Our thesis proposal clearly describes how to include the slack bus and to incorporate the new state variable $\Delta\omega$ into the power flow. It calculates the steady state system frequency after all the generation hits their limits. We validate our long term system frequency calculation by comparing the results with the PSS/E extended term dynamic simulation.

CHAPTER II

POWER FLOW METHOD

The Newton - Raphson method is an iterative approach involving numerical analysis to get a solution that is within an acceptable tolerance. It enables us to replace the nonlinear set of power-flow equations with a linear set. Its key idea is to use sequential linearization.

For Newton - Raphson power flow method, we try to use NR method to find the solution for voltage magnitude and voltage angle at each bus in the system.

2.1 Power Flow Equation

First we have the complex power equation:

$$S_i = V_i I_i^* \quad (1)$$

The Equation (1) above defines the complex power S_i consumed or injected at bus i , which equals to the product of voltage V_i and current I_i conjugate. Here S_i is the complex power at bus i , V_i is the voltage at bus i and I_i^* is the bus i current injection I_i conjugate.

From the Kirchhoff laws, we know that, at a bus i the current injection I_i should equals to the current that flows into the network. So we have:

$$I_i = I_{Gi} - I_{Di} = \sum_{k=1}^n I_{ik} \quad (2)$$

In Equation (2), I_{Gi} is the current injection to bus i from the generator; I_{Di} is the current flows into the load which is connected to bus i ; I_{ik} is the current flows to bus k from bus i .

From the node equations, the current injection at each bus in an N bus system can be written together as:

$$\begin{bmatrix} I_1 \\ I_2 \\ \vdots \\ I_n \end{bmatrix} = \begin{bmatrix} Y_{11} & Y_{12} & \cdots & Y_{1n} \\ Y_{21} & Y_{22} & \cdots & Y_{2n} \\ \vdots & \vdots & \cdots & \vdots \\ Y_{n1} & Y_{n2} & \cdots & Y_{nn} \end{bmatrix} \begin{bmatrix} V_1 \\ V_2 \\ \vdots \\ V_n \end{bmatrix} \quad (3)$$

In this equation, the diagonal term Y_{ii} is the self-admittance of bus i . It equals to the sum of all the admittances that connect to bus i , the summation comes from the Kirchhoff current law. The non-diagonal term Y_{ij} is the negative mutual admittance between bus i and bus j , in which the negative comes from the voltage differences between bus i and j and the ohm's law. I_i is the bus i phase current injection that flows into the network and V_i is the phase voltage to ground at bus i .

2.1.1 Admittance Matrix

Note that Equation (3) defines the admittance matrix Y_{bus} , which is the building stone to find power flow equations. The admittance matrix Y_{bus} defines the relation between the voltage at a bus and the current injection I flows into the same bus.

Here let's use a simple example to illustrate how to create an admittance matrix. Consider a 4-bus system shown as below in Figure 1.

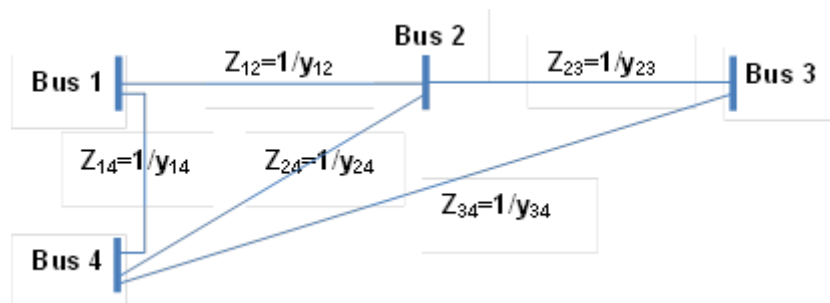


Figure 1 A 4-bus System

Z_{ij} is the branch impedance between bus i and bus j, and y_{ij} is the branch admittance between bus i and bus j. The relation between Z_{ij} and y_{ij} is: $Z_{ij}=1/y_{ij}$. (But the Z has nothing to do with impedance matrix.)

Recalling the Kirchoff's current laws and Ohm's law, we have:

$$I_1 = I_{12} + I_{14} = \frac{V_1 - V_2}{Z_{12}} + \frac{V_1 - V_4}{Z_{14}} = (V_1 - V_2)y_{12} + (V_1 - V_4)y_{14} \quad (4)$$

In Equation (4), I_1 is the current injection at bus 1, I_{12} is the branch current between bus 1 and bus 2, and I_{14} is the branch current between bus 1 and bus 4.

Rearranging Equation (4):

$$I_1 = V_1(y_{12} + y_{14}) + V_2(-y_{12}) + V_4(-y_{14}) \quad (5)$$

Similarly, for the other three buses:

$$I_2 = V_1(-y_{12}) + V_2(y_{12} + y_{23} + y_{24}) + V_3(-y_{23}) + V_4(-y_{24}) \quad (6)$$

$$I_3 = V_2(-y_{23}) + V_3(y_{23} + y_{34}) + V_4(-y_{34}) \quad (7)$$

$$I_4 = V_1(-y_{14}) + V_2(-y_{24}) + V_3(-y_{34}) + V_4(y_{14} + y_{24} + y_{34}) \quad (8)$$

Write these equations together in a matrix form:

$$\begin{bmatrix} I_1 \\ I_2 \\ I_3 \\ I_4 \end{bmatrix} = \begin{bmatrix} y_{12} + y_{14} & -y_{12} & 0 & -y_{14} \\ -y_{12} & y_{12} + y_{23} + y_{24} & -y_{23} & -y_{24} \\ 0 & -y_{23} & y_{23} + y_{34} & -y_{34} \\ -y_{14} & -y_{24} & -y_{34} & y_{14} + y_{24} + y_{34} \end{bmatrix} \begin{bmatrix} V_1 \\ V_2 \\ V_3 \\ V_4 \end{bmatrix} \quad (9)$$

The matrix in Equation (9) which contains branch admittance is called the admittance matrix.

$$Y_{bus} = \begin{bmatrix} y_{12} + y_{14} & -y_{12} & 0 & -y_{14} \\ -y_{12} & y_{12} + y_{23} + y_{24} & -y_{23} & -y_{24} \\ 0 & -y_{23} & y_{23} + y_{34} & -y_{34} \\ -y_{14} & -y_{24} & -y_{34} & y_{14} + y_{24} + y_{34} \end{bmatrix} \quad (10)$$

If we define the elements in Y_{bus} as Y_{ij} , then:

$$\begin{aligned}
 Y_{bus} &= \begin{bmatrix} Y_{11} & Y_{12} & Y_{13} & Y_{14} \\ Y_{21} & Y_{22} & Y_{23} & Y_{24} \\ Y_{31} & Y_{32} & Y_{33} & Y_{34} \\ Y_{41} & Y_{42} & Y_{43} & Y_{44} \end{bmatrix} \\
 &= \begin{bmatrix} y_{12} + y_{14} & -y_{12} & 0 & -y_{14} \\ -y_{12} & y_{12} + y_{23} + y_{24} & -y_{23} & -y_{24} \\ 0 & -y_{23} & y_{23} + y_{34} & -y_{34} \\ -y_{14} & -y_{24} & -y_{34} & y_{14} + y_{24} + y_{34} \end{bmatrix}
 \end{aligned} \tag{11}$$

And Equation (9) can be rewritten as:

$$\begin{bmatrix} I_1 \\ I_2 \\ I_3 \\ I_4 \end{bmatrix} = \begin{bmatrix} Y_{11} & Y_{12} & Y_{13} & Y_{14} \\ Y_{21} & Y_{22} & Y_{23} & Y_{24} \\ Y_{31} & Y_{32} & Y_{33} & Y_{34} \\ Y_{41} & Y_{42} & Y_{43} & Y_{44} \end{bmatrix} \begin{bmatrix} V_1 \\ V_2 \\ V_3 \\ V_4 \end{bmatrix} \tag{12}$$

Y_{ij} are not branch admittances. They are the admittance matrix elements.

This admittance matrix Y_{bus} :

1. It is a symmetric sparse matrix. Y_{ij} equals Y_{ji} .

2. The non-diagonal element Y_{ij} is the negative of branch admittance y_{ij} . It is known as the mutual admittance.

3. The diagonal element Y_{ii} is the sum of all the branch admittances that connect to bus i .

It is also known as the self-admittance.

4. The sum of all the elements in a row or a column is zero.

If we expand the 4-bus system to an N bus system, the admittance matrix can be expressed as:

$$Y_{bus} = \begin{bmatrix} Y_{11} & Y_{12} & \cdots & Y_{1n} \\ Y_{21} & Y_{22} & \cdots & Y_{2n} \\ \vdots & \vdots & \ddots & \vdots \\ Y_{n1} & Y_{n2} & \cdots & Y_{4n} \end{bmatrix} \quad (13)$$

Similarly using Kirchhoff's current law and Ohm's law:

$$\begin{bmatrix} I_1 \\ I_2 \\ \vdots \\ I_n \end{bmatrix} = \begin{bmatrix} Y_{11} & Y_{12} & \cdots & Y_{1n} \\ Y_{21} & Y_{22} & \cdots & Y_{2n} \\ \vdots & \vdots & \ddots & \vdots \\ Y_{n1} & Y_{n2} & \cdots & Y_{4n} \end{bmatrix} \begin{bmatrix} V_1 \\ V_2 \\ \vdots \\ V_n \end{bmatrix} \quad (14)$$

If we define the a current vector $I = \begin{bmatrix} I_1 \\ I_2 \\ \vdots \\ I_n \end{bmatrix}$ and a voltage vector $V = \begin{bmatrix} V_1 \\ V_2 \\ \vdots \\ V_n \end{bmatrix}$. Then

Equation (13) can be simplified as: $I = Y_{bus} V$.

So as an element of vector I, the current injection I_i can be expressed as:

$$I_i = \sum_{k=1}^n I_{ik} = \sum_{k=1}^n Y_{ik} V_k.$$

Then the network equation is:

$$S_i = V_i \left(\sum_{k=1}^n Y_{ik} V_k \right)^* = V_i \sum_{k=1}^n Y_{ik}^* V_k^* \quad (15)$$

Now let's derive Equation (15) into a set of equivalent equations with only real numbers.

Defining: $Y_{ij} = G_{ij} + jB_{ij}$; $V_i = |V_i| \angle \theta_i$; $\theta_{ij} = \theta_i - \theta_j$. Here, G_{ij} is the real part of admittance matrix element Y_{ij} and B_{ij} is the imaginary part of Y_{ij} ; $|V_i|$ is the voltage magnitude at bus i; θ_{ij} is the angle difference between bus i and bus j.

Resolve Equation (15) into real and reactive power part, we have an equivalent set of network equations:

$$\begin{cases} \Phi(|V_i|, \theta_i) = |V_i| \sum |V_j| (G_{ij} \sin \theta_{ij} + B_{ij} \cos \theta_{ij}) \\ \Psi(|V_i|, \theta_i) = |V_i| \sum |V_j| (G_{ij} \sin \theta_{ij} - B_{ij} \cos \theta_{ij}) \end{cases} \quad (16)$$

In Equation (16), $\Phi(|V_i|, \theta_i)$ is the real part network equation, and $\Psi(|V_i|, \theta_i)$ is the reactive part network equation.

On the other side, we can calculate the net injection from the generation and the connected load at each bus:

$$\begin{cases} P_i = P_{Gi} - P_{Di} \\ Q_i = Q_{Gi} - Q_{Di} \end{cases} \quad (17)$$

In Equation (17), P_i is the real power net injection. Q_i is the reactive power net injection. P_{Gi} and Q_{Gi} are real and reactive power generator outputs at bus i . P_{Di} and Q_{Di} are real and reactive demands which are connected to bus i .

Since power system is a balanced system, the net injection power at a bus i should be equal to the transmission network power at bus i . Thus the basic power flow equations in polar form at the bus i can be expressed as:

$$\begin{cases} P_{Gi} - P_{Di} = |V_i| \sum |V_j| (G_{ij} \sin \theta_{ij} + B_{ij} \cos \theta_{ij}) \\ Q_{Gi} - Q_{Di} = |V_i| \sum |V_j| (G_{ij} \sin \theta_{ij} - B_{ij} \cos \theta_{ij}) \end{cases} \quad (18)$$

For any bus i , there are two power flow equations and 4 variables: $|V_i|$, θ_i , P_i and Q_i . If 2 variables are specified, then the other 2 unknown variables will be determined by the 2 power flow equations. Note that $|V_i|$, θ_i are the state variables, which imply if we know the state variables for all buses, we can find all the power flows at all branches. However, not all state variables are unknown variables. Some are regulated by the engineering needs, which become known variables.

Consider an N -bus system. Assume Bus 1 to be the slack bus with a regulated voltage magnitude and angle reference; Bus 2 to Bus $(N-m)$ are PQ buses and Bus $(N-m+1)$ to Bus n are

PV buses. Thus we have 1 slack bus, (N-m-1) PQ buses and m PV buses. In this system, we have 2N power flow equations and 2N unknown variables. However, in the iterative equations, we only need to find the unknown state variables. The remaining unknown variables can be found directly from the power balance equations.

A PV bus is known as a generator bus. At a PV bus, the voltage magnitude is regulated at a specific value. The known variables are voltage magnitude $|V_{sch}|$ and real power net injection P_i ; the unknown variables are reactive power net injection Q_i and voltage angle θ_i . Under this situation, in the iteration we don't need to involve the reactive power balance equations. The reactive power part Q_i can be calculated after the iteration. We have 1 state variable θ and 1 iterative equation for PV bus.

A PQ bus is known as a load bus. At this bus, the real power P_i and Q_i are known and θ and $|V|$ are unknown. We have 2 state variables ($\theta, |V|$) and 2 iterative equations.

A slack bus is a relatively big generator bus that has enough capacity to cover the line losses. In conventional Newton - Raphson method, it will not be involved in the iteration. The P_i and Q_i will be calculated after a convergent solution is found. The voltage magnitude is regulated and the voltage angle is considered to be a reference angle to other bus angles.

So for iterative equations in an N bus system (Bus 1 is slack bus, Bus 2 to Bus (N-m) are PQ buses and Bus (N-m+1) to Bus n are PV buses), there are (2N-2-m) state variables and (2N-2-m) iterative equations in the conventional power flow method.

2.2 Newton - Raphson Method

Now the problem of solving power flow equations boils down to solving non-linear equations: $f(x) = 0$.

The key idea of Newton - Raphson method is to linearize the non-linear equations $f(x)=0$ and then to find the solution x .

For multi-variable Newton - Raphson problem, we consider an m -dimension non-linear

equation set $f(x) = \begin{bmatrix} f_1(x) \\ \vdots \\ f_m(x) \end{bmatrix}$ with an m -dimension state variable vector $x = \begin{bmatrix} x_1 \\ \vdots \\ x_m \end{bmatrix}$.

Here we define $\Delta x^k = x^{k+1} - x^k = \begin{bmatrix} x_1^{k+1} - x_1^k \\ \vdots \\ x_m^{k+1} - x_m^k \end{bmatrix}$.

x^k is the solution of state variable solution after k th iteration; Δx^k is the difference between x^k and x^{k+1} , which improves the solution through the k th iteration process.

We also define the final solution of $f(x)$ as $x_f = \begin{bmatrix} x_{1f} \\ \vdots \\ x_{mf} \end{bmatrix}$, so that $f(x_f) = 0$.

Thus we can use the Taylor's expansion on $f(x)$:

$$f(x) = \left\{ \begin{array}{l} f_1(x^k) + \frac{\partial f_1(x)}{\partial x_1} \Delta x_1^k + \dots + \frac{\partial f_1(x)}{\partial x_m} \Delta x_m^k + \text{higherorder} \\ \vdots \\ f_m(x^k) + \frac{\partial f_m(x)}{\partial x_1} \Delta x_1^k + \dots + \frac{\partial f_m(x)}{\partial x_m} \Delta x_m^k + \text{higherorder} \end{array} \right\} = 0 \quad (19)$$

If we approximate $f(x)$ by ignoring the higher order terms in Equation (19):

$$\begin{aligned}
f(x) &= \begin{bmatrix} f_1(x^k) \\ \vdots \\ f_m(x^k) \end{bmatrix} + \begin{bmatrix} \frac{\partial f_1(x)}{\partial x_1} \Delta x_1^k + \dots + \frac{\partial f_1(x)}{\partial x_m} \Delta x_m^k \\ \vdots \\ \frac{\partial f_m(x)}{\partial x_1} \Delta x_1^k + \dots + \frac{\partial f_m(x)}{\partial x_m} \Delta x_m^k \end{bmatrix} \\
&= \begin{bmatrix} f_1(x^k) \\ \vdots \\ f_m(x^k) \end{bmatrix} + \begin{bmatrix} \frac{\partial f_1(x)}{\partial x_1} & \dots & \frac{\partial f_1(x)}{\partial x_m} \\ \vdots & \ddots & \vdots \\ \frac{\partial f_m(x)}{\partial x_1} & \dots & \frac{\partial f_m(x)}{\partial x_m} \end{bmatrix} \begin{bmatrix} \Delta x_1^k \\ \vdots \\ \Delta x_m^k \end{bmatrix} \approx 0
\end{aligned} \tag{20}$$

The $m \times m$ dimension partial derivative matrix is the Jacobian matrix as follows.

$$J(x) = \begin{bmatrix} \frac{\partial f_1(x)}{\partial x_1} & \dots & \frac{\partial f_1(x)}{\partial x_m} \\ \vdots & \ddots & \vdots \\ \frac{\partial f_m(x)}{\partial x_1} & \dots & \frac{\partial f_m(x)}{\partial x_m} \end{bmatrix} \tag{21}$$

Rearrange Equation (20), we get:

$$\Delta x^k = \begin{bmatrix} \Delta x_1^k \\ \vdots \\ \Delta x_m^k \end{bmatrix} = -J(x)_{x^k}^{-1} \begin{bmatrix} f_1(x^k) \\ \vdots \\ f_m(x^k) \end{bmatrix} \tag{22}$$

The $(k+1)$ th iteration solution is $x^{k+1} = \Delta x^k + x^k$. This solution is closer to the final solution than the k th solution.

If the stop criterion $\|\Delta x^k\| < \varepsilon$ is satisfied now, we can stop and the final solution $x_f = x^{k+1}$ for $f(x)=0$ is found. If the criterion is not satisfied, we should go to next iteration.

$$\text{The iteration is given by: } \left\{ \begin{array}{l} \Delta x^\nu = -J(x)_{x^\nu}^{-1} f(x^\nu) \\ x^{\nu+1} = \Delta x^\nu + x^\nu \end{array} \right\}.$$

Here v is the iteration count. The iteration will stop when either condition reaches the stop criterion: 1) $\|\Delta x^v\| < \varepsilon$; 2) $\|f(x^v)\| < \varepsilon$. A final solution will be obtained when the stop criterion is reached.

2.3 NR Method in Power Flow Analysis

In power flow analysis, we use Newton - Raphson method to determine the voltage angle and voltage magnitude at each bus. Generally, we can use the equation below to express $f(x)$:

$$f(x) = \begin{cases} P_{G0i} - P_{D0i} - |V_i| \sum |V_j| (G_{ij} \sin \theta_{ij} + B_{ij} \cos \theta_{ij}) \\ Q_{G0i} - Q_{D0i} - |V_i| \sum |V_j| (G_{ij} \cos \theta_{ij} - B_{ij} \sin \theta_{ij}) \end{cases} = 0 \quad (23)$$

As we have discussed the unknown variables at each type of bus before, the state variable vector x in an N bus system can be expressed as below:

$$x = \begin{bmatrix} \theta_2 \\ \vdots \\ \theta_n \\ |V_2| \\ \vdots \\ |V_{n-m}| \end{bmatrix} \quad (24)$$

Now let's linearize the power flow equations for each bus by using the Taylor expansion.

$$f_i(x) = \begin{cases} \Delta P_i = P_{Gi} - P_{Di} - \Phi_i(\theta, |V|) \\ \Delta Q_i = Q_{Gi} - Q_{Di} - \Psi_i(\theta, |V|) \end{cases} \quad (25)$$

ΔP_i is defined as the real power mismatch part between network power and net injection at bus i . And ΔQ_i is the reactive power mismatch part at bus i .

Expanding the power flow real power equation by Taylor expansion:

$$\begin{aligned}
& f_i(\theta, |V|) \\
&= f_i(\theta^{(k)}, |V^{(k)}|) + \frac{\partial f_i(\theta, |V|)}{\partial \theta} \Delta \theta^k + \frac{\partial f_i(\theta, |V|)}{\partial |V|} \Delta |V|^k + \text{higherorder} \\
&= P_{Gi} - P_{Di} - \Phi_i(\theta^{(k)}, |V^{(k)}|) + \frac{\partial \Delta P_i}{\partial \theta} \Big|_{\theta^k} \Delta \theta_2^k + \dots + \frac{\partial \Delta P_i}{\partial \theta_n} \Big|_{\theta^k} \Delta \theta_n^k \\
&+ \frac{\partial \Delta P_i}{\partial |V_2|} \Big|_{\theta^k} \Delta |V_2|^k + \dots + \frac{\partial \Delta P_i}{\partial V_n} \Big|_{\theta^k} \Delta |V_n|^k + \text{higherorder} = 0
\end{aligned} \tag{26}$$

Linearize and rewrite Equation (26):

$$P_{Gi} - P_{Di} - \Phi_i(\theta^{(k)}, |V^{(k)}|) + \sum_{q=2}^{n-1} \frac{\partial \Delta P_i}{\partial \theta_q} \Big|_{\theta^k} \Delta \theta_q^k + \sum_{q=2}^{n-1} \frac{\partial \Delta P_i}{\partial |V_q|} \Big|_{\theta^k} \Delta |V_q|^k \approx 0 \tag{27}$$

Similarly, for reactive part power flow equation:

$$Q_{Gi} - Q_{Di} - \Psi_i(\theta^{(k)}, |V^{(k)}|) + \sum_{q=2}^{n-1} \frac{\partial \Delta Q_i}{\partial \theta_q} \Big|_{\theta^k} \Delta \theta_q^k + \sum_{q=2}^{n-1} \frac{\partial \Delta Q_i}{\partial |V_q|} \Big|_{\theta^k} \Delta |V_q|^k \approx 0 \tag{28}$$

Rewrite Equation (27) and Equation (28), we get:

$$\begin{bmatrix} P_{Gi} - P_{Di} - \Phi_i(\theta^{(k)}, |V^{(k)}|) \\ Q_{Gi} - Q_{Di} - \Psi_i(\theta^{(k)}, |V^{(k)}|) \end{bmatrix} + \begin{bmatrix} \frac{\partial \Delta P_i(\theta, |V|)}{\partial \theta} & \frac{\partial \Delta P_i(\theta, |V|)}{\partial |V|} \\ \frac{\partial \Delta Q_i(\theta, |V|)}{\partial \theta} & \frac{\partial \Delta Q_i(\theta, |V|)}{\partial |V|} \end{bmatrix} \begin{bmatrix} \Delta \theta^k \\ \Delta |V|^k \end{bmatrix} \approx 0 \tag{29}$$

The iteration is given by:

$$\begin{bmatrix} \Delta \theta^k \\ \Delta |V|^k \end{bmatrix} = - \begin{bmatrix} \frac{\partial \Delta P_i(\theta, |V|)}{\partial \theta} & \frac{\partial \Delta P_i(\theta, |V|)}{\partial |V|} \\ \frac{\partial \Delta Q_i(\theta, |V|)}{\partial \theta} & \frac{\partial \Delta Q_i(\theta, |V|)}{\partial |V|} \end{bmatrix}_{(\theta^k, |V^k|)}^{-1} \begin{bmatrix} P_{Gi} - P_{Di} - \Phi_i(\theta^{(k)}, |V^{(k)}|) \\ Q_{Gi} - Q_{Di} - \Psi_i(\theta^{(k)}, |V^{(k)}|) \end{bmatrix} \tag{30}$$

$$\text{and } \begin{bmatrix} \theta^{v+1} \\ |V|^{v+1} \end{bmatrix} = \begin{bmatrix} \theta^v + \Delta \theta^v \\ |V|^v + \Delta |V|^v \end{bmatrix}.$$

Here v is the iteration count. The iteration will stop when either condition reaches the

stop criterion: 1) $\|(\Delta \theta^k, \Delta |V^k|)\| < \varepsilon$; 2) $\|f(x^k)\| < \varepsilon$.

So for a power system, the iterative equations at each bus are:

PV bus only has 1 state variable θ and 1 iterative equation and the unknown reactive power net injection Q_i will be calculated after the iteration.

PQ bus has 2 state variables ($\theta, |V|$) and 2 iterative equations.

The slack bus will not be involved in the iteration. The P_i and Q_i will be calculated after a convergent solution is found.

So for iterative equations in the N bus system there are $(2N-2-m)$ state variables and $(2N-2-m)$ iterative equations in the conventional power flow method.

Thus we can get a linear set of iterative equations in a matrix form:

$$\begin{bmatrix} \Delta P_2 \\ \vdots \\ \Delta P_n \\ \Delta Q_2 \\ \vdots \\ \Delta Q_{n-m} \end{bmatrix} = \begin{bmatrix} \frac{\partial \Delta P_2}{\partial \theta_2} & \dots & \frac{\partial \Delta P_2}{\partial \theta_n} & \frac{\partial \Delta P_2}{\partial |V_2|} & \dots & \frac{\partial \Delta P_2}{\partial |V_{n-m}|} \\ \vdots & \ddots & \vdots & \vdots & \ddots & \vdots \\ \frac{\partial \Delta P_n}{\partial \theta_2} & \dots & \frac{\partial \Delta P_n}{\partial \theta_n} & \frac{\partial \Delta P_n}{\partial |V_2|} & \dots & \frac{\partial \Delta P_n}{\partial |V_{n-m}|} \\ \frac{\partial \Delta Q_2}{\partial \theta_2} & \dots & \frac{\partial \Delta Q_2}{\partial \theta_n} & \frac{\partial \Delta Q_2}{\partial |V_2|} & \dots & \frac{\partial \Delta Q_2}{\partial |V_{n-m}|} \\ \vdots & \ddots & \vdots & \vdots & \ddots & \vdots \\ \frac{\partial \Delta Q_{n-m}}{\partial \theta_2} & \dots & \frac{\partial \Delta Q_{n-m}}{\partial \theta_n} & \frac{\partial \Delta Q_{n-m}}{\partial |V_2|} & \dots & \frac{\partial \Delta Q_{n-m}}{\partial |V_{n-m}|} \end{bmatrix} \begin{bmatrix} \theta_2 \\ \vdots \\ \theta_n \\ |V_2| \\ \vdots \\ |V_{n-m}| \end{bmatrix} \quad (31)$$

This partial derivative matrix is the Jacobian matrix.

Here the matrix dimension size is $(2N-2-m) \times (2N-2-m)$. In this iterative matrix, the PQ bus generates 2 rows corresponding to ΔP_i and ΔQ_i ; however the PV bus only generates 1 row corresponding to ΔP_i . And the slack bus 1 is not involved in the iterative matrix.

Simplified Equation (31), we can get:

$$\begin{bmatrix} \Delta P \\ \Delta Q \end{bmatrix} = \begin{bmatrix} H & N \\ M & L \end{bmatrix} \begin{bmatrix} \Delta \theta \\ \Delta |V| \end{bmatrix} \quad (32)$$

H is an (N-1)*(N-1) matrix, it can be expressed as: $H = \begin{bmatrix} \frac{\partial \Phi}{\partial \theta} \end{bmatrix}$. N is an (N-1)*(N-m-1)

matrix, it can be expressed as: $N = \begin{bmatrix} \frac{\partial \Phi}{\partial |V|} \end{bmatrix}$. M is an (N-m-1)*(N-1) matrix, it can be

expressed as: $M = \begin{bmatrix} \frac{\partial \psi}{\partial \theta} \end{bmatrix}$. L is an (N-m-1)*(N-m-1) matrix, it can be expressed as:

$$L = \begin{bmatrix} \frac{\partial \psi}{\partial |V|} \end{bmatrix}.$$

And the iterative matrix in Newton - Raphoson method is called Jacobian matrix:

$$J = \begin{bmatrix} H & N \\ M & L \end{bmatrix} \quad (33)$$

To conclude, the basic power flow procedure is:

1. Set the count number v= 0;
2. Make an initial guess ($\theta^0, |V^0|$) of voltage magnitude and angle at each bus;
3. Compute the network real and reactive power $\Phi(\theta^0, |V^0|)$ and $\psi(\theta^0, |V^0|)$;
4. Compute the real and reactive power mismatch part at each bus:

$$\Delta P_i = P_i - \Phi_i(\theta^{(0)}, |V^{(0)}|) \text{ and } \Delta Q_i = Q_i - \Psi_i(\theta^{(0)}, |V^{(0)}|)$$

5. Update the Jacobian matrix elements, including dimension changes introduced by PV and PQ bus changes.
6. Solve for $\Delta\theta$ and $\Delta|V|$.
7. Calculate the PV bus reactive power Q_{Gi} . Check if the Q_{Gi} is within the generator reactive power limit.

If yes, no change is needed.

If no, Q_{Gi} should be fixed to its limit (Q_{Gi} should be equal to its maximum value, if it is larger than the maximum value; in the other cases, Q_{Gi} should be equal to its minimum value). And this PV bus becomes a PQ bus.

8. Check if the stop criterion is reached.
9. If no, go to next iteration and the count number $v=v+1$. If yes, then stop. A convergent solution is found.

When the iteration count reaches the maximum count limit, the iteration should be stopped and no solution is found.

10. If a convergent solution is found, calculate all the injected power and the slack bus power P_i and Q_i .

CHAPTER III

THEORETICAL FRAMEWORK

3.1 Frequency Stability

In the power system, the ability to recover from a small or a big disturbance, and settle down to an equilibrium state is crucial and essential. The most important two parameters in the system are voltage and system frequency. Maintaining these parameters to be within their tolerances is a very important requirement to power system operation. And frequency in a synchronous power system will be the same in steady state. In the United States, the nominal system frequency is 60 Hz for all the AC power systems and electrical devices. According to IEEE, a frequency that is within ± 0.036 Hz around the nominal frequency can be considered as nominal [8].

The system frequency would be maintained around its nominal frequency if the power supply and the power demand are balanced in the system. When there is a mismatch between power supply and the demand, the frequency deviation starts to occur and the whole system becomes unstable. The system frequency will drop if the supply can't cover the demand and there is no enough reserved generation; otherwise, the system frequency will increase.

Frequency should remain at its nominal value (60 Hz or 50 Hz) because:

Most of the generators and electrical devices are designed to work best at the nominal value. Thus, a non-nominal system frequency will result in the reduction of outputs, lower efficiency of loads and a lower equality of the delivered electrical energy. To some sensitive loads, even a small frequency deviation can be a disaster.

To steam turbines, their stability is highly related to the speed change and they are designed to operate within a very small deviation around the nominal frequency. A steam turbine

blade can't withstand a frequency deviation larger than 2Hz for more than an hour in its entire life [9].

An imbalance between the outputs and loads can be catastrophic to the entire power system. It may result in system black outs, equipment damage and the frequency collapse. And the frequency deviation is an important indicator of the imbalance and the system operating state.

3.2 Frequency Control

The objective of frequency control is to maintain the system frequency close to the nominal value. Thus If there is a disturbance or a mismatch in the system, the frequency control can restore the system frequency back to the nominal frequency quickly.

3.2.1 Frequency Control Structure

The objective of frequency control is to maintain the system frequency close to the nominal value. Thus If there is a disturbance or a mismatch in the system, the frequency control can restore the system frequency back to the nominal frequency quickly.

In the following two sections, the control structure which can ensure the system frequency to be at its nominal value will be described. Usually, this control system mainly consists of the primary control part and the secondary control part. The basic control structures are described by Equation (34):

$$\Delta P_M = \Delta P_C - \frac{1}{R} \Delta \omega \quad (34)$$

In Equation (34), ΔP_M is the mechanical power output, ΔP_C is the set point of steam input, $\Delta \omega$ is the frequency deviation and the R is the droop characteristic.

The primary control is an immediate control change corresponding to the sudden change of load. This control action is usually done at a local power plant level. It is known as droop control. The droop control can make an increase in mechanical power with a lower frequency in order to gain the balance for the system when the system loads increase.

The secondary control is the change in setting control power to maintain operating frequency [10]. This control is also called load frequency control. The reference set point of the steam input of the turbine-governor is adjusted to compensate the large load increment part.

The secondary loop control only exists when the generator has spinning reserves. If the generator has no spinning reserve that means the reference set point has reached its maximum value, the secondary loop control will not work and only the primary control exists in the frequency control.

3.2.2 Primary Control

The primary control is implemented through the turbine-governor to help balance the system. It starts within seconds when the system demands increase and it try to prevent a further frequency deterioration by decrease the frequency to gain a new balance.

Thus when there is an imbalance, primary control will increase the mechanical power to regain the balance by lower the frequency. If there is no secondary loop control, the relation between mechanical increments and frequency decrements are proportional. The droop R is the slope of frequency power characteristics.

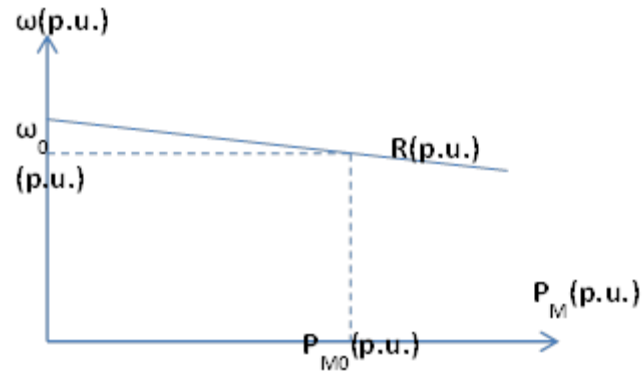


Figure 2 Droop Characteristic

$$\Delta P_M = -\frac{1}{R} \Delta \omega \quad (35)$$

From Figure 2 and Equation (35) shown above, it is obvious to see the droop control allow the system frequency to decrease as the real power demand load increases. The droop control makes a trade-off between the frequency accuracy and the system real power balance. Although this level of control helps cover the power balance in the system, it results in the frequency deviating from the nominal frequency.

However, we should be clear that the primary control only aims to prevent further frequency deterioration and it will not help bring back the system frequency to the nominal rate. Its role is trying to stabilize the frequency as well as to secure a safe system operation. This control responds very fast to the disturbance because it is done at a local level and it does not communicate with other generators or the control center.

3.2.2.1 Droop Characteristics

The basic generator model including turbine-governor system is shown below:

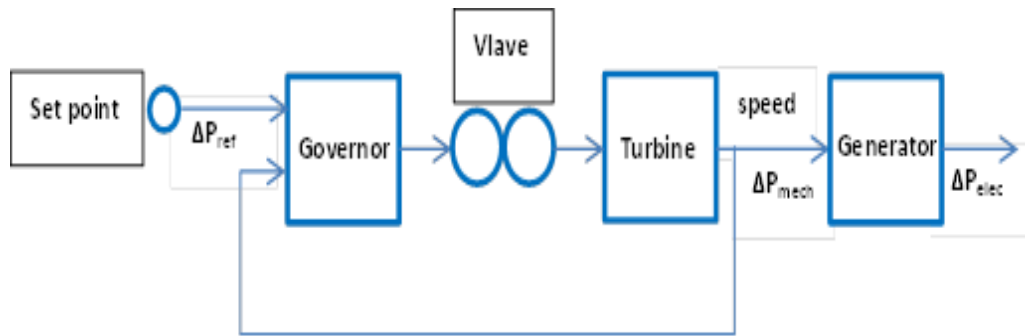


Figure 3 Turbine-Governor Generator System

As we discussed before, the droop characteristic is a ratio between the change in mechanical power and the change in speed. When a mismatch between real power output and load demand in the system occurs, the turbine will first change the speed correspondingly. The governor then will sense this change by receiving the speed feedback and adjust the valve position, in order to make a change to the mechanical power and to gain the power balance. After this process, the mismatch in real power will be zero, however, the speed deviation remains.

From Figure 3, we can see that, in order to provide a given load change, a generator with a less droop will require a smaller speed change than will a generator with a greater generator droop value. Thus the greater the droop is, the less sensitive speed governor system will be.

A good control system should ensure that any load fluctuation ΔP would only produce a small speed change $\Delta\omega$ [11]. It can be achieved by making the droop characteristic R small.

Although droop control helps ensure the system balance, the speed error still exists. The secondary control can offset this error by changing the reference set point, which will be introduced in the next section.

3.2.3 Secondary Control

The secondary control is implemented by adding a supplementary control loop to the turbine–governor system [12]. This loop adds a control signal to the load reference point. The control signal is proportional to the integral of the frequency deviation.

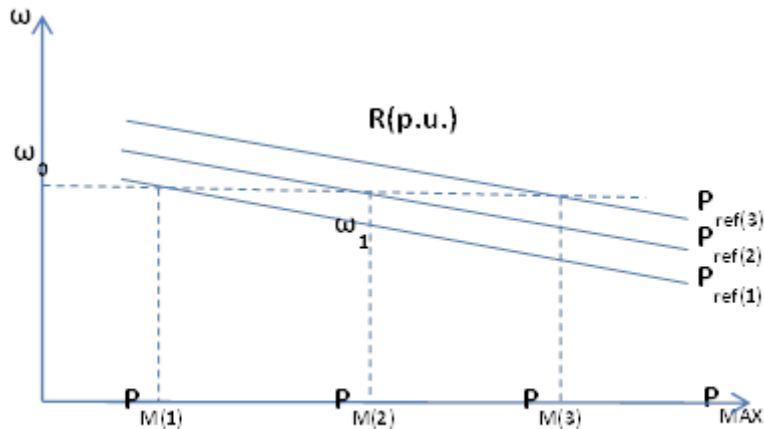


Figure 4 Secondary Loop Control

Figure 4 shows how the secondary loop control usually works to bring the system frequency back to a nominal value. The changes in the settings $P_{ref(1)}$, $P_{ref(2)}$ and $P_{ref(3)}$ enforce a corresponding shift of the characteristic to the positions $P_{m(1)}$, $P_{m(2)}$ and $P_{m(3)}$ [13].

For example, now the desired mechanical power is $P_{m(2)}$, the reference set point of the turbine-governor is $P_{ref(1)}$ and the primary control has driven the system frequency to ω_1 . In order to restore the frequency, the reference set point should be increased. And according to Figure 4, if we move the set point $P_{ref(1)}$ to $P_{ref(2)}$, the mechanical power will be able to cover the demand increments and the frequency will be at its nominal value.

Obviously reference set point has its maximum value P_{MAX} which means the set point of the turbine-governor reaches its maximum position and no more mechanical power can be provided by changing the reference set point position. Before P_{ref} reaches its maximum value, the process of P_{ref} moving upwards P_{MAX} helps increase the total mechanical power and decrease the frequency deviation. This control action is commonly referred to as the secondary loop control on the turbine-governing systems.

Unlike the primary control, the secondary loop control aims to drive the frequency deviation to zero and restore the system frequency. But eventually, when P_{ref} hits its maximum limit, the secondary loop control will be saturated and only primary control is functional in the system.

Details about the turbine-governor model will be introduced in Section 4.2 Dynamic Model

3.3 A Novel Power Flow Method

This section will mainly discuss how to solve a power flow problem at the system frequency level. Details about how to incorporate the frequency deviation as a state variable in power flow method will be introduced.

Power flow calculation is one of the most important operations in power system. It is used to determine the steady-state operation of an electric power system. It calculates the voltage magnitude and angle at each bus, the power flow in all branch and feeder circuits and the line losses in transmission lines.

In power system, Newton - Raphson method is widely used to get power flow solution for a system. It is fast converged and accurate. However, the conventional Newton - Raphson method is operated under 2 assumptions:

a. The generations are enough to cover the load. The slack bus can always cover the mismatch part of the system.

b. Frequency is considered to be steady at 60 Hz.

In fact, the generator real power output of slack bus has its maximum value and the system frequency is a variable which is related to the generator and load model. The present power flow methods just allow us to calculate static vector under a normal power system state. When the real power outputs cannot cover the load demands in the system under some abnormal conditions, the conventional power flow will not be able to describe the system.

3.3.1 Generator Model and Load Model

The relation between frequency deviation and the models of generators and loads will be introduced in this section.

3.3.1.1 Generator Model

In this novel power flow method, the system is under an abnormal condition that is all the generators' real power outputs have reached their limits. In this situation, the secondary loop control is saturated and there will be only primary control. We should also assume that the mechanical power from turbine equals the generated power from PV bus here.

Thus the system frequency deviation affects the units real power generation, mainly due to the droop characteristics R. The generator i real power output part can be described as:

$$P_{Gi} = P_{G0i} [1 - K_{Gi} \Delta\omega] \quad (36)$$

Where, P_{Gi} is the real power output of the generator i;

P_{G0i} is the nominal value of the above variable;

K_{Gi} is the frequency characteristic coefficient of the generator i real power output.

K_{Gi} can be also interpreted as the inverse of droop characteristic R. ($K_{Gi} = 1/R$)

Equation (36) describes the relation between generated real power and frequency deviation. However, the reactive power output of a generator is still determined under the condition that the magnitude of $|V_{sch}|$ equals its regulated value.

3.3.1.2 Load Model

Common static load models for active and reactive power are expressed in a polynomial or an exponential form, and can include a frequency dependence term if it is necessary. In this study, in order to simplify the whole power flow model, all the load models are voltage dependent in a polynomial form, such as constant impedance model, constant current model and constant power model.

Depending on the power relation to the voltage, the static characteristics of the load can be classified into constant power (P), constant current (I) and constant impedance (Z) load model.

The ZIP model is the combination of these three models. Equation (37) and Equation (38) represent the ZIP model in a polynomial form:

$$P_{Li} = P_{Loi} \left[a_1 \left(\frac{|V_i|}{|V_0|} \right)^2 + a_2 \left(\frac{|V_i|}{|V_0|} \right) + a_3 \right] \quad (37)$$

$$Q_{Li} = Q_{Loi} \left[a_1 \left(\frac{|V_i|}{|V_0|} \right)^2 + a_2 \left(\frac{|V_i|}{|V_0|} \right) + a_3 \right] \quad (38)$$

$$a_1 + a_2 + a_3 = 1 \quad (39)$$

Where $|V_0|$, P_0 and Q_0 are the initial state values of the studying power system, and the coefficients a_1 , a_2 and a_3 are the parameters of the model.

For a constant impedance load, the power dependence on voltage is quadratic. It is used to describe some lighting load and a_1 is the coefficient parameter of this model.

For a constant current load model, its change is linear with voltage. It is used to describe a load demand mixed of motor devices and resistive and a_2 is the coefficient parameter of this model.

For a constant power the power it is independent of changes in voltage. In conventional power flow method, this voltage invariant load model is used and a_3 is the coefficient parameter of this model.

3.3.2 State Variables

In this section, we will focus on the state variables in both conventional power flow method and the novel power flow method. As we discussed in Section 2.2, the system frequency control usually consists of primary control and secondary control. When the outputs of all generators in a system hit their limits, that is, the reference set points reach their maximum values; there will be only droop control. Under this condition, the system will be operating in an abnormal state and the system frequency will deviate from its nominal value.

Thus the previous assumptions of conventional power flow will not be acceptable now:

- a. The system frequency is no more a constant.
- b. Slack bus concept needs to be adapted to frequency changes.
 - a) With an additional state variable $\Delta\omega$, one more iterative equation in power flow is needed.
 - b) The slack bus now should also be involved in the power flow calculation. But it is still needed to be the voltage angle reference.

Frequency deviation, $\Delta\omega$ is now considered as new state variable in power flow and it will be incorporated in the power flow equations. This variable is related to the real power balance.

For an N-bus system in conventional power flow method, assume there are (m) PV buses; the number of PQ bus will be (N-1-m).

For the slack bus, P_G and Q_G are unknown. They are not involved in the iterative equations. They just need to be calculated after the power flow found a convergent solution.

For PV bus, the real power P_G and $|V_{sch}|$ are known and θ is unknown. Since there are (m) PV buses in the system, we have (m) unknown voltage angles θ and (m) iterative equations for PV buses.

For PQ bus, the real power P_G and Q_G are known and θ and $|V|$ are unknown. Since there are (N-1-m) PQ buses in the system, we have (N-1-m) unknown voltage angles θ , (N-1-m) unknown voltage magnitudes $|V|$ and $2(N-1-m)$ iterative equations for PQ buses.

In total, there are $(m)+(N-1-m)+(N-1-m)=(2N-2-m)$ unknown variables and $(m)+2(N-1-m)=(2N-2-m)$ iterative equations in power flow for conventional Newton - Raphson method.

However, if we introduce frequency deviation as a new state variable to the power flow equations, the situation will be different. We need to have one more iterative equation because now we have an additional variable in power flow. As we stated before, frequency should be incorporated in the power flow when all the generator output limits have been reached, the real power of slack bus is no longer an unknown variable in the system. It equals to its maximum generation value.

For an N-bus system in novel power flow method, when all the generators hit their limits:

For the system, the system frequency deviation $\Delta\omega$ is an unknown variable.

For the slack bus, P_G is known since it equals to its maximum generation value. And it will be included in the iterative equation. However, the Q_G is still unknown.

For PV bus, the real power P_G and $|V_{sch}|$ are known and θ is unknown. Since there are (m) PV buses in the system, we have (m) unknown voltage angles θ and (m) iterative equations for PV buses.

For PQ bus, the real power P_G and Q_G are known and θ and $|V|$ are unknown. Since there are (N-1-m) PQ buses in the system, we have (N-1-m) unknown voltage angles θ , (N-1-m) unknown voltage magnitudes $|V|$ and $2(N-1-m)$ iterative equations for PQ buses.

In total, there are $(1)+(m)+(N-1-m)+(N-1-m)=(2N-1-m)$ unknown variables and $(1)+(m)+2(N-1-m)=(2N-1-m)$ iterative equations in the novel power flow method.

The variables of conventional NR method and PFLTFS method are shown in Table 1 below.

Table 1 State Variables

| | PV Bus | PQ Bus | Slack Bus | $\Delta\omega$ |
|---------------------------|---|---|---|--|
| Conventional NR Method | P , V (known) Q , θ(unknown) | P , Q (known) V , θ(unknown) | P , Q (unknown) Not included in the iterative equations | Fixed known value |
| PFLTFS Method | P , V (known) Q , θ(unknown) | P , Q (known) V , θ(unknown) | P (known) and it is included in the iterative equations Q(unknown) and it is not included in the iterative equations | New State Variable |

3.3.3 The PFLTFS Method

3.3.3.1 The PF Equations in Novel Power Flow Method

As the assumption mentioned before, in this study we consider frequency deviation as a new state variable and load model to be voltage dependent.

Calculate network equation using Kirchhoff laws and Ohm's law:

$$S_i = V_i \sum_{k=1}^n Y_{ik}^* V_k^* \quad (40)$$

Y_{ik} is the mutual admittance between bus i and bus k . Equation (40) describes the transmission network equation with complex numbers.

Now let's derive this equation into a set of equivalent equations with only real numbers.

Defining: $Y_{ij} = G_{ij} + jB_{ij}$, $V_i = |V_i| \angle \theta_i$; $\theta_{ij} = \theta_i - \theta_j$. Here, G_{ij} is the real part of admittance matrix element Y_{ij} and B_{ij} is the imaginary part of Y_{ij} ; $|V_i|$ is the voltage magnitude at bus i ; θ_{ij} is the angle difference between bus i and bus j .

Resolve Equation (40) into real and reactive power part, we have an equivalent set of network equations:

$$\left\{ \begin{array}{l} \Phi_i(\theta, V) = \sum_{k=1}^n |V_k| |V_i| (G_{ik} \cos \theta_{ik} + B_{ik} \sin \theta_{ik}) \\ \Psi_i(\theta, V) = \sum_{k=1}^n |V_k| |V_i| (G_{ik} \sin \theta_{ik} - B_{ik} \cos \theta_{ik}) \end{array} \right\} \quad (41)$$

In Equation (41), define the function $\Phi_i(|V_i|, \theta_i)$ as the real power part and the function $\Psi_i(|V_i|, \theta_i)$ as the reactive power part. They are same to the conventional power flow method.

On the other side, we can calculate the net injection from the generation and the connected load at each bus:

$$\left\{ \begin{array}{l} P_i = P_{Gi} - P_{Di} = P_{GMAXi}[1 - K_{Gi}\Delta\omega] - P_{D0i}\left[a_1\left(\frac{|V_i|}{|V_0|}\right)^2 + a_2\left(\frac{|V_i|}{|V_0|}\right) + a_3\right] \\ Q_i = Q_{Gi} - Q_{Di} = Q_{Gi} - Q_{D0i}\left[a_1\left(\frac{|V_i|}{|V_0|}\right)^2 + a_2\left(\frac{|V_i|}{|V_0|}\right) + a_3\right] \end{array} \right\} \quad (42)$$

In Equation (42), P_i is the real power net injection. Q_i is the reactive power net injection. P_{Gi} and Q_{Gi} are real and reactive power generator outputs at bus i . P_{Di} and Q_{Di} are real and reactive demands which are connected to bus i . K_{Gi} is the inverse of generator droop characteristic R_i at bus i .

The modifications are:

1. The frequency deviation now is related to the generator droop characteristics. Then in order to incorporate frequency deviation in power flow, we need to modify the PV bus power flow equation by replacing the P_{Gi} (the constant generated real power from bus- i) with $P_{GMAXi}[1 - K_{Gi}\Delta\omega]$ (the generator output with a droop characteristic). P_{GMAXi} equals the generator output limit at bus i .

Now the real power outputs are larger than the output limits at PV buses, which seems violating the generator output limit; however, the exceeded amount is extracted from rotation energy. That is how the droop control works to obtain a system balance through frequency reduction.

Since the frequency deviation only affects the real power, the reactive output power Q_{Gi} remains the same.

2. In addition, as we introduced before, load models in this study are voltage dependent. So the P_{Li} and Q_{Li} should also be modified. Given the ZIP load model in polynomial form below:

$$P_{Di} = P_{D0i}\left[a_1\left(\frac{|V_i|}{|V_0|}\right)^2 + a_2\left(\frac{|V_i|}{|V_0|}\right) + a_3\right] \quad (37)$$

$$Q_{Di} = Q_{D0i} [a_1 (\frac{|V_i|}{|V_0|})^2 + a_2 (\frac{|V_i|}{|V_0|}) + a_3] \quad (38)$$

$$a_1 + a_2 + a_3 = 1 \quad (39)$$

P_{D0i} and Q_{D0i} are the real and reactive part of the demand at bus i before the units tripping.

Then the power flow equations in novel method can be described as:

$$\left\{ \begin{array}{l} \sum_{k=1}^n |V_k| |V_i| (G_{ik} \cos \theta_{ik} + B_{ik} \sin \theta_{ik}) = P_{GMAXi} [1 - K_{Gi} \Delta \omega] - P_{D0i} [a_1 (\frac{V_i}{V_0})^2 + a_2 (\frac{V_i}{V_0}) + a_3] \\ \sum_{k=1}^n |V_k| |V_i| (G_{ik} \sin \theta_{ik} - B_{ik} \cos \theta_{ik}) = Q_{G0i} - Q_{D0i} [a_1 (\frac{V_i}{V_0})^2 + a_2 (\frac{V_i}{V_0}) + a_3] \end{array} \right\} \quad (43)$$

For any bus i , there are two power flow equations and 4 variables: $|V_i|$, θ_i , P_i and Q_i . If two variables are specified, then the other 2 unknown variables will be determined by the 2 power flow equations.

Consider an N -bus system, we have $2N$ power flow equations and $2N$ unknown variables. However, in the iterative equations, we only need to find out the unknown state variables. The remaining unknown variables can be found directly from the power balance equations.

In the novel power flow method:

1. Since the system outputs cannot cover the demands, all the generator outputs in PFLTFS are directly considered to be equal to the generator maximum output value. And only primary control will be included in the calculation.

It cannot be denied that there is a dynamic process when both the primary control and the secondary control exist. However, all the output limits will be reached, the I-

controller will finally be saturated, and only the primary control will exist. Thus we bypassed the period when secondary loop control exists, and directly compute the steady state power flow solution with the primary control.

The PFLTFS method only cares about finding the final static power flow solution including the system frequency. That is why it is a much faster and easier way to find the abnormal state system power flow.

2. For the system:

a. There is a new unknown state variable $\Delta\omega$ -- frequency deviation.

b. For PV bus, the voltage magnitude is regulated at a specific value. The known variables are voltage magnitude $|V_{sch}|$ and real power net injection P_i ; the unknown variables are reactive power net injection Q_i and voltage angle θ_i . Under this situation, in the iteration we don't need to involve the reactive power balance equations. The reactive power part Q_i can be calculated after the iteration. We have 1 unknown state variable θ and 1 iterative equation for PV bus.

c. For PQ bus, the real power P_i and Q_i are known and θ and $|V|$ are unknown. We have 2 unknown state variables ($\theta, |V|$) and 2 iterative equations.

d. For slack bus, the real power output $P_{Gislack}$ is known. According to point 1 mentioned above, the real power output should equals to the generator maximum output value. That is $P_{Gislack}=P_{GMAXslack}$. And $P_{Gislack}$ will be involved in the iteration. The reactive power part Q_{islack} will still be calculated after a convergent solution is found. The voltage magnitude is regulated and the angle is considered to be a reference angle to other bus angles. The slack bus will provide an extra equation in the novel power flow method.

So for iterative equations in the N bus system (Bus 1 is slack bus, Bus 2 to Bus (N-m) are PQ buses and Bus (N-m+1) to Bus n are PV buses), there are (2N-1-m) state variables and (2N-1-m) iterative equations in the novel power flow method.

3.3.3.2 Iterative Equations in Novel Power Flow Method

In novel power flow method, we still need to find a convergent solution of the non-linear power flow equations $f(x)$ that satisfies the power system balance.

$$f(x) = \left\{ \begin{array}{l} P_{GMAXi} [1 - K_{Gi} \Delta\omega] - P_{D0i} [a_1 (\frac{V_i}{V_0})^2 + a_2 (\frac{V_i}{V_0}) + a_3] - V_i \sum V_j (G_{ij} \sin \theta_{ij} + B_{ij} \cos \theta_{ij}) \\ Q_{G0i} - Q_{D0i} [a_1 (\frac{V_i}{V_0})^2 + a_2 (\frac{V_i}{V_0}) + a_3] - V_i \sum V_j (G_{ij} \sin \theta_{ij} - B_{ij} \cos \theta_{ij}) \end{array} \right\} \quad (44)$$

where, P_{GMAXi} equals the generator output limit at bus i;

Q_{G0i} is the generated reactive power from bus i;

P_{D0i} and Q_{D0i} are the real and reactive part of the demands at bus i before the units tripping.

We can use ΔP_i and ΔQ_i to express the real and reactive mismatch power parts at bus i as below:

$$\left\{ \begin{array}{l} \Delta P_i(\theta, |V|) = P_{GMAXi}(\Delta\omega) - P_{Di}(|V|) - \Phi_i(\theta, |V|) \\ \Delta Q_i(\theta, |V|) = Q_{Gi}(\Delta\omega) - Q_{Di}(|V|) - \Psi_i(\theta, |V|) \end{array} \right\} \quad (45)$$

As we have discussed the unknown variables at each type of bus before, the unknown state variable vector x in the N-bus system can be expressed as below:

$$x = \begin{bmatrix} \theta_2 \\ \vdots \\ \theta_n \\ |V_2| \\ \vdots \\ |V_{n-m}| \\ \omega \end{bmatrix} \quad (46)$$

Now let's find the iterative equations in PFLTFS method:

For PQ bus, we have 2 state variables (θ , $|V|$) and 2 equations in the iteration.

$$\left\{ \begin{array}{l} \Delta P_i = -P_{L0i} \left[a_1 \left(\frac{|V_i|}{|V_0|} \right)^2 + a_2 \left(\frac{|V_i|}{|V_0|} \right) + a_3 \right] - |V_i| \sum |V_j| (G_{ij} \sin \theta_{ij} + B_{ij} \cos \theta_{ij}) \\ \Delta Q_i = -Q_{L0i} \left[a_1 \left(\frac{|V_i|}{|V_0|} \right)^2 + a_2 \left(\frac{|V_i|}{|V_0|} \right) + a_3 \right] - |V_i| \sum |V_j| (G_{ij} \cos \theta_{ij} - B_{ij} \sin \theta_{ij}) \end{array} \right\} \quad (47)$$

For PV bus, we have 1 unknown state variable θ and only 1 equation.

$$\begin{aligned} \Delta P_i &= P_{GMAXi} [1 - K_{Gi} \Delta \omega] - P_{L0i} \left[a_1 \left(\frac{|V_i|}{|V_0|} \right)^2 + a_2 \left(\frac{|V_i|}{|V_0|} \right) + a_3 \right] \\ &- |V_i| \sum |V_j| (G_{ij} \sin \theta_{ij} + B_{ij} \cos \theta_{ij}) \end{aligned} \quad (48)$$

For slack bus, it will provide an extra equation in the novel power flow method.

$$\begin{aligned} \Delta P_{slack} &= P_{GMAXslack} [1 - K_{Gslack} \Delta \omega] - P_{L0slack} \left[a_1 \left(\frac{V_{slack}}{V_0} \right)^2 + a_2 \left(\frac{V_{slack}}{V_0} \right) + a_3 \right] \\ &- V_{slack} \sum V_j (G_{slackj} \sin \theta_{slackj} + B_{slackj} \cos \theta_{slackj}) \end{aligned} \quad (49)$$

Then there are $(2N-1-m)$ unknown state variables and $(2N-1-m)$ equations in the novel power flow method iteration.

So the iterative equations in a matrix form can be expressed as:

$$\begin{bmatrix} \Delta P_{slack} \\ \Delta P_2 \\ \vdots \\ \Delta P_n \\ \Delta Q_2 \\ \vdots \\ \Delta Q_{n-m} \end{bmatrix} = \begin{bmatrix} \frac{\partial \Delta P_{slack}}{\partial \theta_2} & \dots & \frac{\partial \Delta P_{slack}}{\partial \theta_n} & \frac{\partial \Delta P_{slack}}{\partial |V_2|} & \dots & \frac{\partial \Delta P_{slack}}{\partial |V_{n-m}|} & \frac{\partial \Delta P_{slack}}{\partial \Delta \omega} \\ \frac{\partial \Delta P_2}{\partial \theta_2} & \dots & \frac{\partial \Delta P_2}{\partial \theta_n} & \frac{\partial \Delta P_2}{\partial |V_2|} & \dots & \frac{\partial \Delta P_2}{\partial |V_{n-m}|} & \frac{\partial \Delta P_2}{\partial \Delta \omega} \\ \vdots & \ddots & \vdots & \vdots & \ddots & \vdots & \vdots \\ \frac{\partial \Delta P_n}{\partial \theta_2} & \dots & \frac{\partial \Delta P_n}{\partial \theta_n} & \frac{\partial \Delta P_n \Phi_n}{\partial |V_2|} & \dots & \frac{\partial \Delta P_n}{\partial |V_{n-m}|} & \frac{\partial \Delta P_n}{\partial \Delta \omega} \\ \frac{\partial \Delta Q_2}{\partial \theta_2} & \dots & \frac{\partial \Delta Q_2}{\partial \theta_n} & \frac{\partial \Delta Q_2}{\partial |V_2|} & \dots & \frac{\partial \Delta Q_2}{\partial |V_{n-m}|} & \frac{\partial \Delta P_{n-m}}{\partial \Delta \omega} \\ \vdots & \ddots & \vdots & \vdots & \ddots & \vdots & \vdots \\ \frac{\partial \Delta Q_{n-m}}{\partial \theta_2} & \dots & \frac{\partial \Delta Q_{n-m}}{\partial \theta_n} & \frac{\partial \Delta Q_{n-m}}{\partial |V_2|} & \dots & \frac{\partial \Delta Q_{n-m}}{\partial |V_{n-m}|} & \frac{\partial \Delta Q_{n-m}}{\partial \Delta \omega} \end{bmatrix} \begin{bmatrix} \theta_2 \\ \vdots \\ \theta_n \\ |V_2| \\ \vdots \\ |V_{n-m}| \\ \Delta \omega \end{bmatrix} \quad (50)$$

Here the matrix dimension size is $(2N-1-m) * (2N-1-m)$. In this iterative matrix, the PQ bus generates 2 rows corresponding to ΔP_i and ΔQ_i ; the PV bus only generates 1 row corresponding to ΔP_i . The slack bus 1 also generates 1 row corresponding to ΔP_{1slack} .

This iterative matrix is a $(2N-1-m) * (2N-1-m)$ dimension matrix.

Simplified Equation (50), we can get:

$$\begin{bmatrix} \Delta P_{slack} \\ \Delta P \\ \Delta Q \end{bmatrix} = J(x) \begin{bmatrix} \Delta \theta \\ \Delta |V| \\ \Delta \omega \end{bmatrix} \quad (51)$$

The iterative matrix $J(x)$ here is called Jacobian matrix. We'll discuss this matrix in details in next section.

These modified power balance equations are different from those used in the conventional NR power flow method. The conventional Newton - Raphson power flow method only relates the real power mismatch parts to voltage magnitudes, and the reactive power mismatch parts to angle differences. In these modified equations, the system frequency deviation is also involved.

3.3.3.3 Jacobian Matrix in Novel Power Flow Method

Now let's try to form the Jacobian matrix in novel power flow method. The novel power flow will still be solved by using the iterative equations below:

$$\begin{bmatrix} \Delta P_{slack} \\ \Delta P_2 \\ \vdots \\ \Delta P_n \\ \Delta Q_2 \\ \vdots \\ \Delta Q_{n-m} \end{bmatrix} = J(x) \begin{bmatrix} \Delta \theta_2 \\ \vdots \\ \Delta \theta_n \\ \Delta |V_2| / |V_0| \\ \vdots \\ \Delta |V_{n-m}| / |V_0| \\ \Delta \omega \end{bmatrix} \quad (52)$$

Since we introduced a new state variable $\Delta \omega$ to the state variables, correspondingly there is an extra real power balance equation from the slack bus.

For the Jacobian matrix in the novel power flow method, the dimension will be increased by adding a column and a row (compared to the conventional Jacobian matrix). Here we describe the augmented Jacobian matrix in a simplified way:

$$\begin{bmatrix} \Delta P_{slack} \\ \Delta P \\ \Delta Q \end{bmatrix} = \begin{bmatrix} \frac{\partial \Delta P_{slack}}{\partial \theta} & \frac{\partial \Delta P_{slack}}{\partial |V|} & \frac{\partial \Delta P_{slack}}{\partial \Delta \omega} \\ \frac{\partial \Delta P_i}{\partial \theta} & \frac{\partial \Delta P_i}{\partial |V|} & \frac{\partial \Delta P_i}{\partial \Delta \omega} \\ \frac{\partial \Delta Q_i}{\partial \theta} & \frac{\partial \Delta Q_i}{\partial |V|} & \frac{\partial \Delta Q_i}{\partial \Delta \omega} \end{bmatrix} \begin{bmatrix} \Delta \theta \\ \Delta |V| \\ \Delta \omega \end{bmatrix} \quad (53)$$

In this augmented Jacobian matrix:

a. For $\frac{\partial \Delta P_i}{\partial \Delta \theta}$, they are the same to the conventional Jacobian elements $\frac{\partial \Delta P_i}{\partial \Delta \theta}$.

$$\frac{\partial \Delta P_i}{\partial \Delta \theta_i} = \sum_{j \neq i} |V_i| |V_j| |Y_{ij}| \sin(\theta_{ij} - \delta_i + \delta_j) \quad (54)$$

$$\frac{\partial \Delta P_i}{\partial \Delta \theta_j} = -|V_i| |V_j| |Y_{ij}| \sin(\theta_{ij} - \delta_i + \delta_j), i \neq j \quad (55)$$

b. For $\frac{\partial \Delta Q_i}{\partial \Delta \theta}$, they are the same to the conventional Jacobian elements $\frac{\partial \Delta Q_i}{\partial \Delta \theta}$.

$$\frac{\partial \Delta Q_i}{\partial \Delta \theta} = \sum_{j \neq i} |V_i| |V_j| |Y_{ij}| \cos(\theta_{ij} - \delta_i + \delta_j) \quad (56)$$

$$\frac{\partial \Delta Q_i}{\partial \Delta \theta_j} = -|V_i| |V_j| |Y_{ij}| \cos(\theta_{ij} - \delta_i + \delta_j), i \neq j \quad (57)$$

c. For $\frac{\partial \Delta P_{slack}}{\partial \Delta \theta}$:

$$\frac{\partial \Delta P_{slack}}{\partial \Delta \theta_j} = -|V_{slack}| |V_j| |Y_{slackj}| \sin(\theta_{slackj} - \delta_{slack} + \delta_j), slacknum \neq j \quad (58)$$

d. For $\frac{\partial \Delta P_i}{\partial \Delta |V|}$ and $\frac{\partial \Delta Q_i}{\partial \Delta |V|}$,

$$\frac{\partial \Delta P_i}{\partial \Delta |V_j|} \text{ and } \frac{\partial \Delta Q_i}{\partial \Delta |V_j|} \text{ are the same to the conventional elements } \frac{\partial \Delta P_i}{\partial \Delta |V_j|} \text{ and } \frac{\partial \Delta Q_i}{\partial \Delta |V_j|}$$

in the Jacobian matrix:

$$\frac{\partial \Delta P_i}{\partial \Delta |V_j|} = |V_i| |Y_{ij}| \cos(\theta_{ij} - \delta_i + \delta_j), i \neq j \quad (59)$$

$$\frac{\partial \Delta Q_i}{\partial \Delta |V_j|} = -|V_i| |Y_{ij}| \sin(\theta_{ij} - \delta_i + \delta_j), i \neq j \quad (60)$$

However, $\frac{\partial \Delta P_i}{\partial |V_i|}$ and $\frac{\partial \Delta Q_i}{\partial |V_i|}$ are different from the conventional Jacobian elements

$\frac{\partial \Delta P_i}{\partial |V_i|}$ and $\frac{\partial \Delta Q_i}{\partial |V_i|}$. As we discussed before, load models are voltage dependent. These load

models will impact the PQ bus real power derivatives of voltage and reactive power derivatives

of voltage. Thus the related elements $\frac{\partial \Delta P_i}{\partial |V_i|}$ and $\frac{\partial \Delta Q_i}{\partial |V_i|}$ in Jacobian matrix should be modified.

For ZIP load model in polynomial form:

$$P_{Li} = P_{L0i} \left[a_1 \left(\frac{|V_i|}{|V_0|} \right)^2 + a_2 \left(\frac{|V_i|}{|V_0|} \right) + a_3 \right] \quad (37)$$

$$Q_{Li} = Q_{L0i} \left[a_1 \left(\frac{|V_i|}{|V_0|} \right)^2 + a_2 \left(\frac{|V_i|}{|V_0|} \right) + a_3 \right] \quad (38)$$

$$a_1 + a_2 + a_3 = 1 \quad (39)$$

So at a PQ bus i, the $\frac{\partial \Delta P_i}{\partial |V_i|}$ and $\frac{\partial \Delta Q_i}{\partial |V_i|}$ should be:

$$\frac{\partial \Delta P_i}{\partial |V_i|} = -2|V_i| G_{ii} - \sum_{\substack{j=1 \\ j \neq i}}^n |V_j| (G_{ij} \cos \theta_{ij} + B_{ij} \sin \theta_{ij}) + a_2 P_0 + 2a_1 P_0 \left(\frac{|V_i|}{|V_0|} \right) \quad (61)$$

$$\frac{\partial \Delta Q_i}{\partial |V_i|} = -\sum_{\substack{j=1 \\ j \neq i}}^n |V_j| (G_{ij} \sin \theta_{ij} - B_{ij} \cos \theta_{ij}) + 2|V_i| B_{ii} + a_2 Q_0 + 2a_1 Q_0 \left(\frac{|V_i|}{|V_0|} \right) \quad (62)$$

Compared to conventional power flow, the elements $\frac{\partial \Delta P_i}{\partial |V_i|}$ and $\frac{\partial \Delta Q_i}{\partial |V_i|}$ are modified by

adding a voltage dependent power part.

e. For $\frac{\partial \Delta P_{slack}}{\partial \Delta |V|}$:

$$\frac{\partial \Delta P_{slack}}{\partial \Delta |V_j|} = -|V_{slack}| |Y_{slackj}| \cos(\theta_{slackj} - \delta_{slack} + \delta_j), slacknum \neq j \quad (63)$$

f. For $\frac{\partial \Delta P_i}{\partial \Delta \omega}$:

$$\text{For PV bus: } \frac{\partial \Delta P_i}{\partial \Delta \omega} = -K_{Gi} P_{G0i} \quad (64)$$

At a PV bus, the generator outputs are related to frequency deviation due to the droop characteristic.

$$\text{For PQ bus: } \frac{\partial \Delta P_i}{\partial \Delta \omega} = 0 \quad (65)$$

$$\text{g. For } \frac{\partial \Delta Q_i}{\partial \Delta \omega} : \frac{\partial \Delta Q_i}{\partial \Delta \omega} = 0 \quad (66)$$

$$\text{h. For } \frac{\partial \Delta P_{slack}}{\partial \Delta \omega} :$$

$$\frac{\partial \Delta P_{slack}}{\partial \Delta \omega} = -K_{Gslack} P_{G0slack} \quad (67)$$

The slack bus provides an extra iterative equation for the system. P_G is known since it equals to its maximum generation value. It is included in the iterative equation. However, the Q_G is still unknown. The system frequency deviation is related to the generator real power output due to the generator's droop characteristics.

In these iterative equations and this augmented Jacobian matrix, the frequency deviation is incorporated. It will be included in the iteration as the other state variables, until the error vector reaches the stop criterion and a solution is found. The Jacobian matrix dimension is increased to $(2N-1-m) \times (2N-1-m)$ in the novel power flow method.

The novel power flow procedure is almost same to conventional power flow procedure. We first set the count number $v=0$ and make an initial guess of $(\theta^0, |V^0|)$. While error vector is larger than the tolerance, do the iteration. And then increase the count number $v=v+1$. The iteration will stop when the tolerance reaches the stop criterion or when the counter reaches the maximum number.

A detailed flow chart of PFLTFS method (Figure 5) will be showed in Section 3.3.4.

3.3.4 The Flow Chart of PFLTFS Method

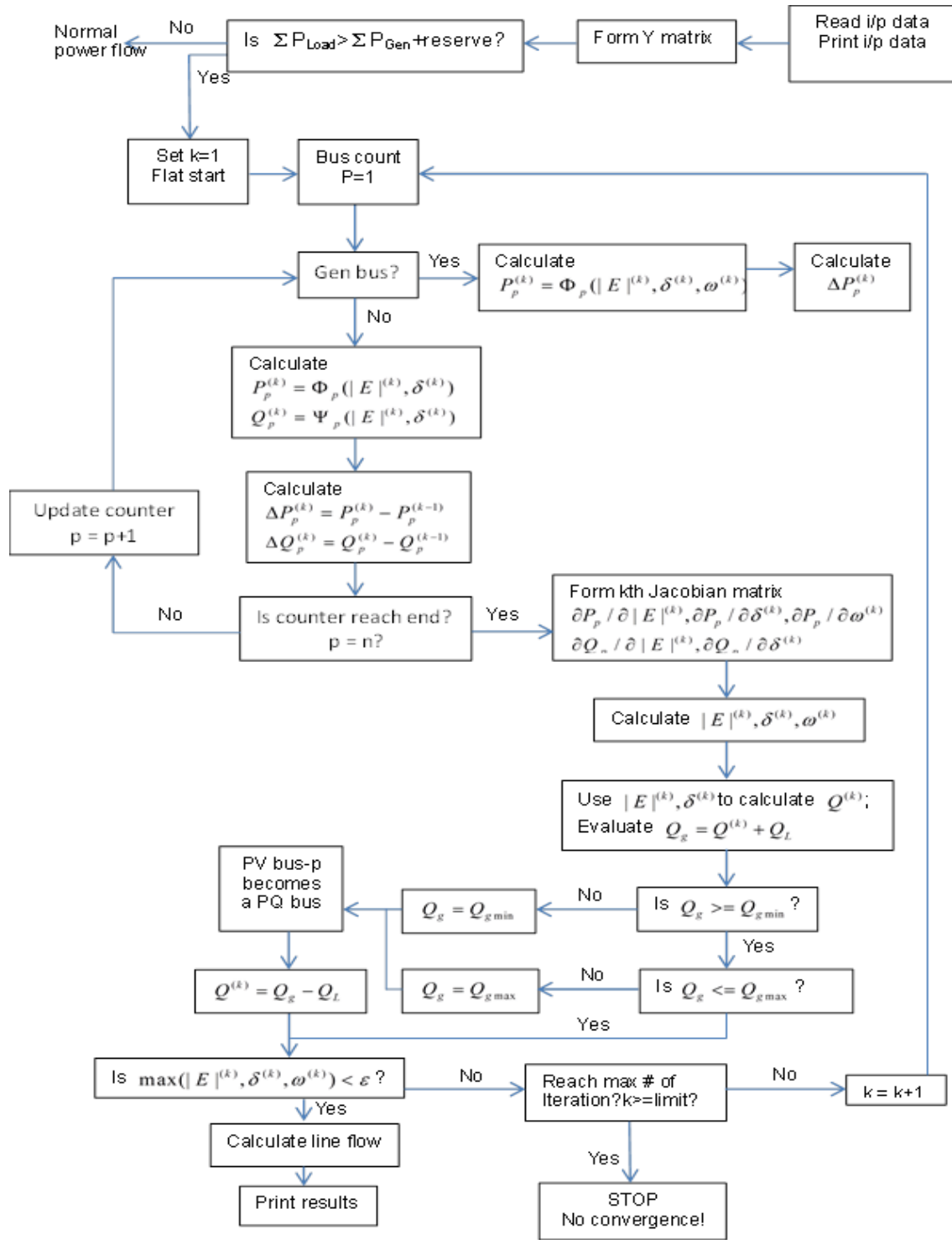


Figure 5 Flow Chart of PFLTFS Method

CHAPTER IV

PSS/E ENVIRONMENT AND DYNAMIC MODEL

4.1 PSS/E Environment

We used the Siemens-PTI's PSS/E simulation tool to conduct power flow and dynamic simulation studies. The Power System Simulator for Engineering or PSS/E is a software tool from Siemens and it is widely used by electrical transmission participants. It is an integrated, interactive program for simulating, analyzing, and optimizing power system performance [14]. It provides the user many advanced methods such as Power Flow, Dynamic Simulation, Fault Analysis and Extended Term Dynamic Simulation. This software is typically used by electrical transmission planners to do analysis and to obtain a reliable power system.

The PSS/E dynamic simulation interface is independent of the PSS/E interface and operated as a separate program. Its dynamic simulation tools provide all the functionality for transient, dynamic and extended term dynamic stability analysis. [15] The dynamic modeling includes modeling the synchronous machine, turbine governor, exciter system, and stabilizer system.

In this study, Power Flow, Dynamic Simulation and Extended Term Dynamic Simulation have been used. All the simulations are operated under PSS/E version 33.

4.1.1 Dynamic Simulation Setup Procedure

This section will give a detailed introduction about how to setup the dynamic simulation in PSS/E step by step.

Step 1: Perform a power flow before the dynamic simulation.

In PSS/E, every dynamic simulation is based on a power flow Saved Case which provides the initial bus data, branch data, machine data and load data. This save case can be derived after we run a power flow for a system whose raw data we have input to PSS/E.

Step 2: Convert the model and data in the Save Case.

This step helps convert the generator models, load models and other data in power flow Saved Case to a dynamic form that can be used in the dynamic simulation. This save case data is used as the initial state for the following dynamic simulation. Four functions will be operated in this step: Convert Loads and Generators; Order Network for Matrix Operations (re-orders the buses and converts the swing bus to a PV bus); Factorize Admittance Matrix and Solution for Switching Studies.

Step 3: Prepare the dynamic data file for dynamic simulation.

This dynamic data file includes the detailed model of the generator systems and other equipment which haven't been included in the power flow case data, such as turbine-governor model, exciter model and stabilizer model.

Step 4: Check consistency and set the output channel

After we prepared the dynamic data file, we should check whether this data file can be used or not. Operate function DYCH (dynamic data file check) to check the data file, and it should say "Consistency Check OK". Then perform CHAN order and choose the parameters we would like to plot after the dynamic simulation.

Step 5: Run a base case dynamic simulation.

Before adding any disturbance to the system, the dynamic simulation should run under a base case to ensure the system is under a normal state at first. Click STRT function, set the simulation time and the output file saved path. Then click RUN to run the dynamic simulation.

Step 6: Add the disturbance and run the simulation.

Choose a disturbance from the Fault menu, and then repeat step 5.

Step 7: Plot the output channel.

Open the output file and drag an output channel from the list to the main screen. Thus we have finished a dynamic simulation [16].

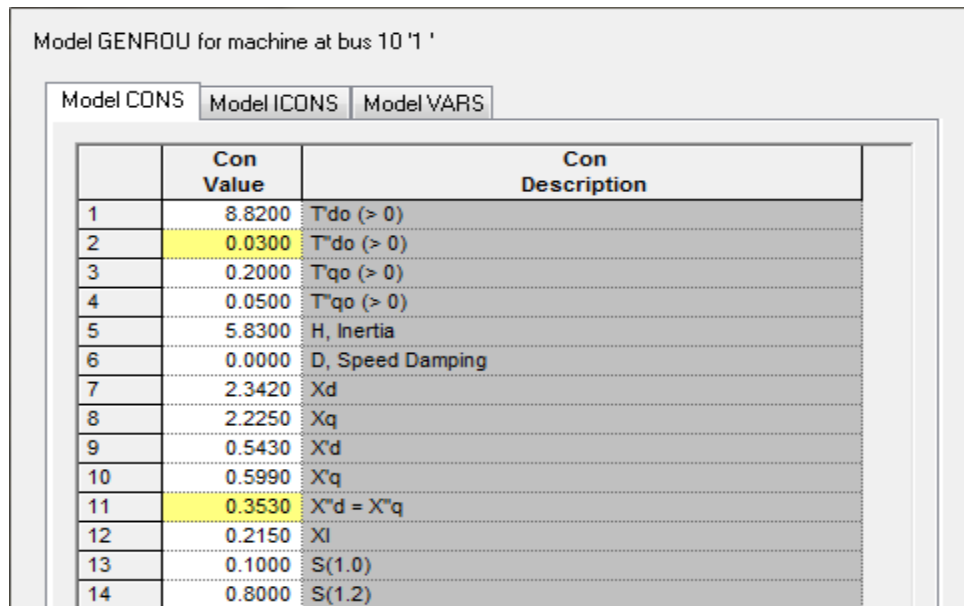
4.2 Dynamic Model

PSS/E generator models ranges from simplest to very complicated models. In this study, GENROU is used as all the generator models.

4.2.1 Generator Model

“GENROU” - round rotor generator model

“GENROU” represent solid rotor generators at the sub transient level. It is a widely used model that has the general characteristics of most generators.



Model GENROU for machine at bus 10 '1'

| | Con Value | Con Description |
|----|-----------|-----------------------------------|
| 1 | 8.8200 | T ^{do} (> 0) |
| 2 | 0.0300 | T ^{do} (> 0) |
| 3 | 0.2000 | T ^{qo} (> 0) |
| 4 | 0.0500 | T ^{qo} (> 0) |
| 5 | 5.8300 | H, Inertia |
| 6 | 0.0000 | D, Speed Damping |
| 7 | 2.3420 | X _d |
| 8 | 2.2250 | X _q |
| 9 | 0.5430 | X' _d |
| 10 | 0.5990 | X' _q |
| 11 | 0.3530 | X ^{*d} = X ^{*q} |
| 12 | 0.2150 | X _I |
| 13 | 0.1000 | S(1,0) |
| 14 | 0.8000 | S(1,2) |

Figure 6 Generator Model Data Sheet

In every model data sheet, there are many parameters and values describing the equipment and its location. These values and parameters are categorized into four types: CON, VAR, STATE and ICON [17]. Only the values in CON are required to be completed for a basic system model setup. A convenient way to fill out the data form is to use the same data from the sample case and then modify some values which are needed to be changed for particular purposes.

The model data sheet of GENROU model which is used in the study is shown above. (Figure 6)

4.2.2 Turbine Governor Model

In this case study steam turbine governor models are used. Both TGOV1 and TGOV5 are used in this dynamic model. All turbine governor data is specified on the base of its generating unit in PSS/E and the governor droop R have the same value for all units in a system to ensure proper load sharing.

TGOV1 is a simplified steam turbine governor model with primary control. (Figure 7)
For output < 100 MW unit: TGOV1 (steam turbine governor)

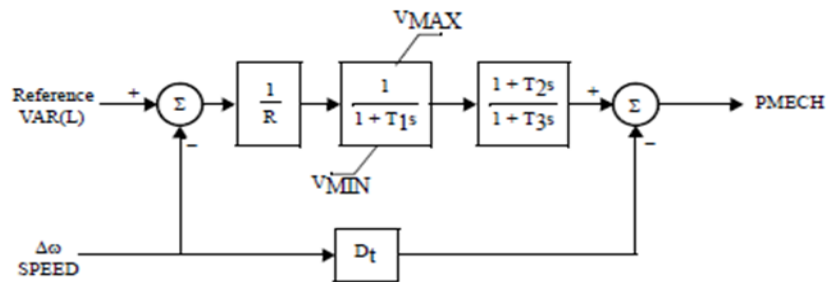


Figure 7 TGOV1 Model [18]

Model TGOV1 for machine at bus 12 '1'

Model CONS Model ICONS Model VARS

| | Con Value | Con Description |
|---|-----------|-----------------|
| 1 | 0.0200 | R |
| 2 | 0.4900 | T1 (>0)(sec) |
| 3 | 100.0000 | V MAX |
| 4 | -100.0000 | V MIN |
| 5 | 2.1000 | T2 (sec) |
| 6 | 7.1234 | T3 (>0)(sec) |
| 7 | 0.0000 | Dt |

Figure 8 TGOV1 Dynamic Data

Figure 8 shows the data in TGOV1 model. The first constant value in TGOV1 is the droop characteristic of the governor.

TGOV5 is a more complicated model with secondary loop control. (Figure 9) For output > 100 MW unit: TGOV5 (1981 IEEE type one governor model modified to include boiler controls) [19].

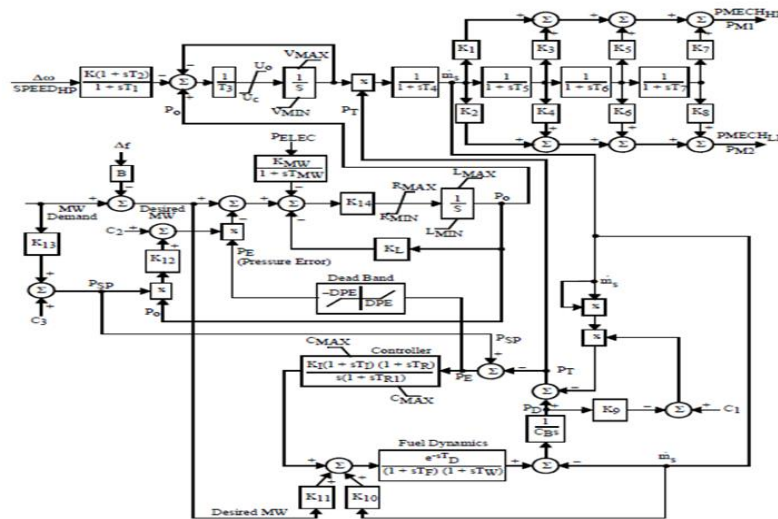


Figure 9 TGOV5 Model [20]

Model TGOV5 for machine at bus 10 '1'

Model CONS Model ICONS Model VARS

| | Con Value | Con Description |
|----|-----------|-----------------|
| 1 | 50.0000 | K |
| 2 | 0.0000 | T1 |
| 3 | 0.0000 | T2 |
| 4 | 0.1500 | T3 (> 0) |
| 5 | 0.4000 | Uo |
| 6 | -0.4000 | Uc (< 0) |
| 7 | 100.0000 | VMAX |
| 8 | -100.0000 | VMIN |
| 9 | 0.4000 | T4 |
| 10 | 0.3000 | K1 |
| 11 | 0.0000 | K2 |
| 12 | 9.0000 | T5 |
| 13 | 0.4000 | K3 |
| 14 | 0.0000 | K4 |
| 15 | 0.5000 | T6 |
| 16 | 0.3000 | K5 |
| 17 | 0.0000 | K6 |
| 18 | 0.0000 | T7 |
| 19 | 0.0000 | K7 |
| 20 | 0.0000 | K8 |
| 21 | 0.0000 | K9 |
| 22 | 0.0000 | K10 |
| 23 | 0.0000 | K11 |
| 24 | 0.0000 | K12 |
| 25 | 0.0000 | K13 |
| 26 | 5.0000 | K14 |
| 27 | 0.5000 | RMAX |
| 28 | -0.5000 | RMIN |
| 29 | 0.4500 | LMAX |
| 30 | 0.0000 | LMIN |
| 31 | 0.2000 | C1 |
| 32 | 0.0000 | C2 |
| 33 | 1.0000 | C3 |
| 34 | 20.0000 | B |
| 35 | 200.0000 | CB (> 0) |
| 36 | 0.0200 | KI |
| 37 | 90.0000 | TI |
| 38 | 60.0000 | TR |
| 39 | 6.0000 | TR1 |
| 40 | 100.0000 | CMAX |
| 41 | -100.0000 | CMIN |
| 42 | 60.0000 | TD |

Figure 10 TGOV5 Dynamic Data

| | | |
|----|---------|---------------------|
| 43 | 25.0000 | TF |
| 44 | 7.0000 | TV |
| 45 | 1.0000 | Psp (Initial) (> 0) |
| 46 | 0.0000 | TMV |
| 47 | 0.0000 | KL (0.0 or 1.0) |
| 48 | 0.0000 | KMW (0.0 or 1.0) |
| 49 | 0.0000 | DPE |

Figure 10 Continued.

TGOV5 is the only steam turbine model in PSS/E that includes secondary loop control. For TGOV5, PSS/E offers four turbine control strategies: Boiler Follow Mode; Turbine Follow Mode; Coordinated Optimal Mode and Variable Pressure Mode.

In this study, we use the **boiler follow mode** typical data. In this mode, changes in generation are initiated by turbine control valves and then boiler controls respond with necessary control action. The turbine has the access to the stored energy in the boiler and load changes occur with **fairly rapid response**.

In Figure 10, most of the data are from the sample case only a few of them are modified. The first constant parameter K is the inverse of the droop, and the two constant parameters in the red circle (Lmax and Lmin) are the output limit value.

4.2.3 Exciter Model

For exciter model, SEXS and IEEET2 have been used in this dynamic model.

Models SEXS represents no specific type of excitation system, but rather the general characteristics of a wide variety of properly tuned excitation systems [21]. For output < 100 MW unit: SEXS (Simplified excitation system model).

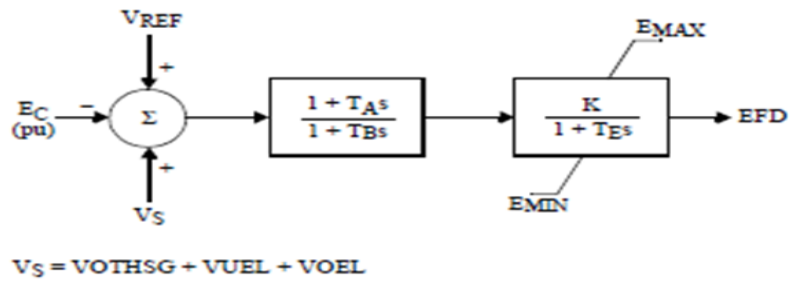


Figure 11 SEXS Exciter Model [22]

Model SEXS is particularly useful to present a simple excitation system with a basic detailed design. (Figure 11) The gain, K , time constant, T_E , and limits E_{MAX} , E_{MIN} , are a basic representation of the excitation power source. Time constants T_A and T_B in Figure 12 provide the transient gain reduction needed to allow satisfactory dynamic behavior with high steady-state gain [23].

Model SEXS for machine at bus 1 '1'

| Con | Value | Description |
|-----|-----------|-------------|
| 1 | 0.1000 | TA/TB |
| 2 | 10.0000 | TB (> 0) |
| 3 | 200.0000 | K |
| 4 | 0.1000 | TE |
| 5 | -100.0000 | EMIN |
| 6 | 100.0000 | EMAX |

Figure 12 SEXS Dynamic Data

Model IEEE2 has an excitation system stabilizing feedback. (Figure 13)

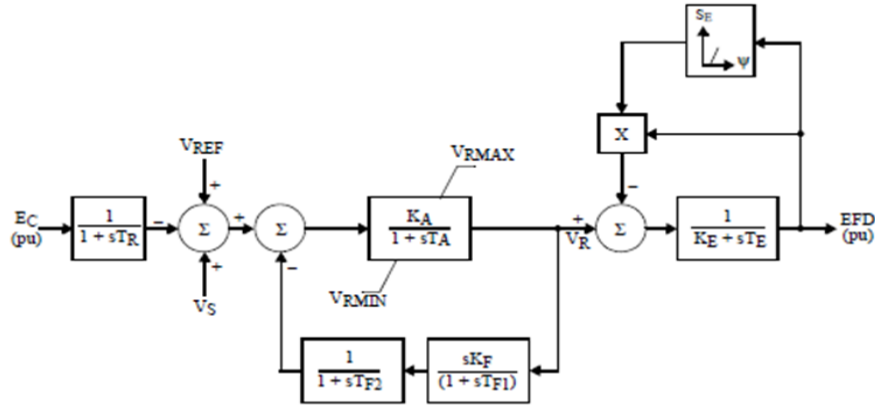


Figure 13 IEEET2 Model [24]

The feedback signal that is used in IEEET2 model is proportional to the control element output. In order to stabilize the voltage quickly after the tripping, IEEET2 model is used for the large output units. For output > 100 MW unit: IEEET2 (1968 IEEE type 2 excitation system model).

Model IEEET2 for machine at bus 10 '1'

Model CONS Model ICONS Model VARS

| | Con Value | Con Description |
|----|-----------|-----------------|
| 1 | 0.0100 | TR (sec) |
| 2 | 300.0000 | KA |
| 3 | 0.0250 | TA (sec) |
| 4 | 16.7000 | VRMAX or zero |
| 5 | -13.4000 | VRMIN |
| 6 | 1.0000 | KE or zero |
| 7 | 0.2900 | TE (>0)(sec) |
| 8 | 0.0200 | KF |
| 9 | 1.0000 | TF1 (>0)(sec) |
| 10 | 0.2900 | TF2 (>0) |
| 11 | 4.6730 | E1 |
| 12 | 1.5700 | SE(E1) |
| 13 | 6.2300 | E2 |
| 14 | 1.6800 | SE(E2) |

Figure 14 IEEET2 Dynamic Data

The dynamic data of the IEEEET2 model is shown in Figure 14.

4.2.4 Stabilizer Models

The stabilizer is a device that injects supplementary signals into the voltage regulator units. Stabilizer output at a machine can be accessed as other signals input by the excitation system model.

Model IEEEEST for machine at bus 10 '1'

Model CONS Model ICONS Model VARS

| | Con Value | Con Description |
|----|-----------|--|
| 1 | 0.0000 | A1 |
| 2 | 0.0000 | A2 |
| 3 | 0.0000 | A3 |
| 4 | 0.0000 | A4 |
| 5 | 0.0000 | A5 |
| 6 | 0.0000 | A6 |
| 7 | 0.3000 | T1 |
| 8 | 0.0500 | T2 |
| 9 | 0.1500 | T3 |
| 10 | 0.0500 | T4 |
| 11 | 0.0000 | T5 (if equal to 0, sT5 will equal 1.0) |
| 12 | 3.0000 | T6 (>= 0) |
| 13 | 7.5000 | KS |
| 14 | 0.3000 | LSMAX |
| 15 | -0.3000 | LSMIN |
| 16 | 0.0000 | VCU (p.u.)(if equal to 0, ignored.) |
| 17 | 0.0000 | VCL (p.u.)(if equal to 0, ignored.) |

Figure 15 IEEEEST Dynamic Data

Model IEEEEST implements a general-purpose supplementary stabilizer representation [25].

It helps ensure that the supplementary signal is zero in the steady state. In order to stabilize the voltage quickly after the tripping, IEEEEST model is used for the large output units.

For output > 100 MW unit: IEEEEST Model (1981 IEEE stabilizer)

The dynamic data of the IEEEEST stabilizer model is shown in Figure 15.

4.3 Frequency Response

Now it is possible to analyze the response of a power system caused by the tripping of a generating unit.

This response can be divided into four stages:

Stage 1: Rotor swings in the generator (first few seconds)

The sudden unit tripping will produce a large rotor swings at the tripping bus and much smaller rotor swings in the other generators in the system.

A unit tripping will cause the mechanical power to drop by the same amount to the unit tripping power. Since the rotor angle cannot change immediately after the disturbance occurs, the electrical power of the generator will be greater than the mechanical power for a while.

Stage 2: Frequency drop (a few seconds)

Stage 1 will last only for a few seconds. After stage 1, the power imbalance starts to cause all the generators to speed down; thus the system frequency begins to drop. In this stage, all the generators will slow down at the same rate if they are remained in synchronism, no matter how far the electrical distance between a generator and the tripping bus is.

Stage 3: Primary control and Secondary control (several seconds to a minute) [26]

As the system frequency drops, the governor receives the feedback signal from the turbine and starts to open the main control valves to increase the turbine mechanical power

output. This increase in mechanical power for each generator is related to the frequency primary control. The frequency decreases in primary control due to the droop R of turbine characteristic.

The secondary loop control usually involves AGC when the tie-lines exist. When the secondary control starts, the central regulator sends control signals to the all the generator units to force them to increase their power output by moving towards the maximum or minimum reference set point. The secondary loop control aims to drive the frequency deviation to zero.

Stage 4: Only droop control (more than 10 minutes)

When the set point reaches its limit, the secondary control will be saturated. There will be only the primary control to help the system to settle down.

CHAPTER V

STUDY CASE MODELING AND SIMULATION

In the conventional power flow, there are two assumptions which cannot be accepted by the power system that is under a droop control. One is the no output limit in the slack bus; another is the system frequency is considered to be steady at 60 Hz. That is why we provide a novel power flow method to do the power flow when the outputs in the system have been reached.

In this chapter, we focus on power flow issues about a system whose generation limits have been reached because of units tripping. How to apply the PFLTFS method to solve this type of power flow will be introduced.

The power flow case studies on a 4-bus small system and on the IEEE 118-bus system will be introduced. The case study will include the static state solution (PFLTFS method) and the PSS/E dynamic simulation solution. To realize the PFLTFS method, a static state power flow simulation was created in Matlab programming environment in this thesis.

5.1 A 4-bus System Case Study

In this section, a small system example will be used to illustrate the modified power flow method.

Consider a 4-bus system in Figure 16: bus-1 and bus-4 are PV buses; bus-2 and bus-3 are PQ buses. In this small system, the generator of bus-4 suddenly shuts down. Try to incorporate frequency deviation into power flow analysis, and find the final solution. The assumptions are shown below:

- a. All the values are uniformed. (The Base MVA is 100 MVA; and the Base Frequency is 60 Hz.)
- b. The droop characteristic ($1/R = K = 30$).
- c. The load is not frequency dependent.
- d. The load model in this case is constant impedance.

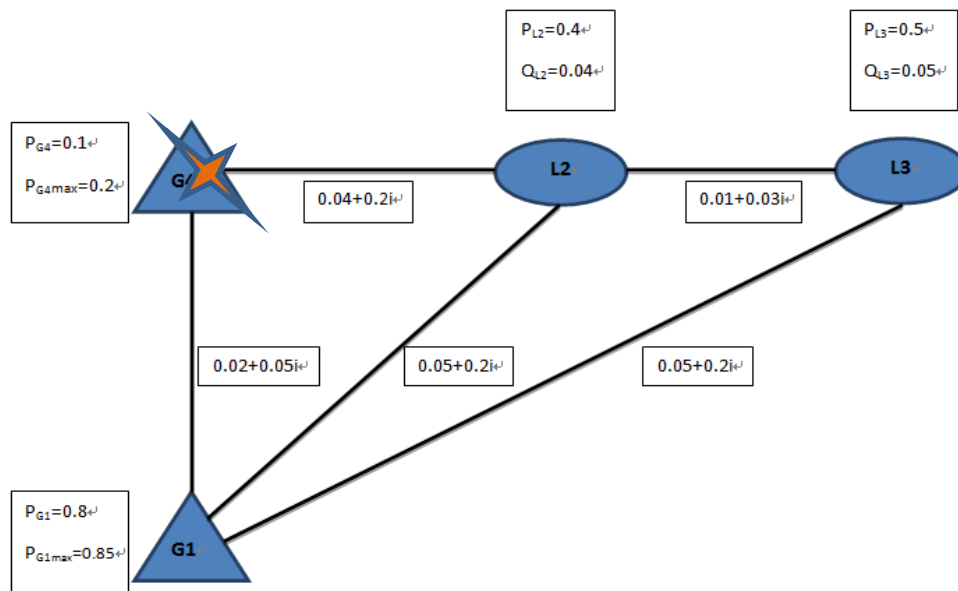


Figure 16 A simple 4-bus System

5.1.1 The PFLTFS Method for Static State Power Flow

When the generator connected to Bus-4 goes off, the generator at Bus-1 has to pick up all the demands. The trip unit is Bus-4 with a 0.1 p.u. output. That is 11% of the total real power generation. The maximum output of Bus-1 is 0.85 p.u.; however, the demands of Bus-2 and Bus-3 are 0.9 p.u. in total.

So the generation limit will be reached. That means the secondary control is saturated and there will be no secondary loop in the generator, only droop control. The frequency

deviation will be included as a new state variable in the power flow equations. (Use Newton - Raphson Method)

a. Step 1: find the system admittance matrix Y.

For Bus-4, because the generator has tripped and there is no other generations or loads connected to this bus, it now can be considered as a PQ bus with $P = 0$ p.u., and $Q = 0$ p.u.

The new Y-matrix is expressed as:

$$Y_{new} = \begin{bmatrix} 9.25 - j26.65 & -1.18 + j4.71 & -1.18 + j4.71 & -6.90 + j17.24 \\ -1.18 + j4.71 & 12.14 - j39.51 & -10.00 + j30.00 & -0.96 + j4.81 \\ -1.18 + j4.71 & -10.00 + j30.00 & -1.18 + j4.71 & 0 \\ -6.90 + j17.24 & -0.96 + j4.81 & 0 & 7.86 - j22.05 \end{bmatrix} \quad (68)$$

b. Step 2: Known and unknown variables

Bus 1: PV bus. This bus used to be a slack bus with an unknown real power output, but now the P_{G1} reaches its limit and it becomes a known variable. Voltage is regulated to 1. This bus is still the angle reference bus.

Bus 2: PQ bus. P_{L2} and Q_{L2} are known; $|V_2|$ and Θ_2 are unknown.

Bus 3: PQ bus. P_{L3} and Q_{L3} are known; $|V_3|$ and Θ_3 are unknown.

Bus 4: PQ bus, $P_{L4} = Q_{L4} = 0$ p.u.; $|V_4|$ and Θ_4 are unknown.

$\Delta\omega$ is a new unknown variable in the power flow equations.

c. Step 3: PF Equations and Iterative Equations

Power Flow Equations:

$$\Delta P_i = P_{Goi} - P_{Loi} - |V_i| \sum |V_j| (G_{ij} \sin \theta_{ij} + B_{ij} \cos \theta_{ij}) \quad (69)$$

$$\Delta Q_i = Q_{Goi} - Q_{Loi} - |V_i| \sum |V_j| (G_{ij} \cos \theta_{ij} - B_{ij} \sin \theta_{ij}) \quad (70)$$

Iterative Equations:

$$\text{Bus 1: } \Delta P_{G1} = P_{G1} - K\Delta\omega - |V_1| \sum |V_j| (G_{1j} \sin \theta_{1j} + B_{1j} \cos \theta_{1j}) \quad (71)$$

$$\text{Bus 2: } \left\{ \begin{array}{l} \Delta P_{L2} = -P_{L2} * \left(\frac{|V_2|}{|V_0|} \right)^2 - |V_2| \sum |V_j| (G_{2j} \sin \theta_{2j} + B_{2j} \cos \theta_{2j}) \\ \Delta Q_{L2} = -Q_{L2} * \left(\frac{|V_2|}{|V_0|} \right)^2 - |V_2| \sum |V_j| (G_{2j} \sin \theta_{2j} - B_{2j} \cos \theta_{2j}) \end{array} \right\} \quad (72)$$

$$\text{Bus 3: } \left\{ \begin{array}{l} \Delta P_{L3} = -P_{L3} * \left(\frac{|V_3|}{|V_0|} \right)^2 - |V_3| \sum |V_j| (G_{3j} \sin \theta_{3j} + B_{3j} \cos \theta_{3j}) \\ \Delta Q_{L3} = -Q_{L3} * \left(\frac{|V_3|}{|V_0|} \right)^2 - |V_3| \sum |V_j| (G_{3j} \sin \theta_{3j} - B_{3j} \cos \theta_{3j}) \end{array} \right\} \quad (73)$$

$$\text{Bus 4: } \left\{ \begin{array}{l} \Delta P_{L4} = -P_{L4} * \left(\frac{|V_4|}{|V_0|} \right)^2 - |V_4| \sum |V_j| (G_{4j} \sin \theta_{4j} + B_{4j} \cos \theta_{4j}) \\ \Delta Q_{L4} = -Q_{L4} * \left(\frac{|V_4|}{|V_0|} \right)^2 - |V_4| \sum |V_j| (G_{4j} \sin \theta_{4j} - B_{4j} \cos \theta_{4j}) \end{array} \right\} \quad (74)$$

In this small system, compared to the conventional iterative equations, the only change here is the slack bus provides an extra iterative equation in the novel method. In a bigger system, all the PV bus real power iterative equations should be modified by adding the droop control part to the equations.

d. Step 4: Jacobian Matrix.

Compared to the conventional Newton - Raphson method, the Jacobian matrix dimension size is augmented from 6*6 to 7*7.

The Jacobian matrix in this 4-bus system can be expressed as:

$$\begin{bmatrix} \Delta P_{G1} \\ \Delta P_{L2} \\ \Delta P_{L3} \\ \Delta P_{L4} \\ \Delta Q_{L2} \\ \Delta Q_{L3} \\ \Delta Q_{L4} \end{bmatrix} = \begin{bmatrix} \frac{\partial \Delta P_{G1}}{\partial \Delta \theta_2} & \frac{\partial \Delta P_{G1}}{\partial \Delta \theta_3} & \frac{\partial \Delta P_{G1}}{\partial \Delta \theta_4} & \frac{\partial \Delta P_{G1}}{\partial \Delta |V_2|} |V_0| & \frac{\partial \Delta P_{G1}}{\partial \Delta |V_3|} |V_0| & \frac{\partial \Delta P_{G1}}{\partial \Delta V_4} |V_0| & -K \\ \frac{\partial \Delta P_{L2}}{\partial \Delta \theta_2} & \frac{\partial \Delta P_{L2}}{\partial \Delta \theta_3} & \frac{\partial \Delta P_{L2}}{\partial \Delta \theta_4} & \frac{\partial \Delta P_{L2}}{\partial \Delta |V_2|} |V_0| & \frac{\partial \Delta P_{L2}}{\partial \Delta |V_3|} |V_0| & \frac{\partial \Delta P_{L2}}{\partial \Delta V_4} |V_0| & 0 \\ \frac{\partial \Delta P_{L3}}{\partial \Delta \theta_2} & \frac{\partial \Delta P_{L3}}{\partial \Delta \theta_3} & \frac{\partial \Delta P_{L3}}{\partial \Delta \theta_4} & \frac{\partial \Delta P_{L3}}{\partial \Delta |V_2|} |V_0| & \frac{\partial \Delta P_{L3}}{\partial \Delta |V_3|} |V_0| & \frac{\partial \Delta P_{L3}}{\partial \Delta V_4} |V_0| & 0 \\ \frac{\partial \Delta P_{L4}}{\partial \Delta \theta_2} & \frac{\partial \Delta P_{L4}}{\partial \Delta \theta_3} & \frac{\partial \Delta P_{L4}}{\partial \Delta \theta_4} & \frac{\partial \Delta P_{L4}}{\partial \Delta |V_2|} |V_0| & \frac{\partial \Delta P_{L4}}{\partial \Delta |V_3|} |V_0| & \frac{\partial \Delta P_{L4}}{\partial \Delta V_4} |V_0| & 0 \\ \frac{\partial \Delta Q_{L2}}{\partial \Delta \theta_2} & \frac{\partial \Delta Q_{L2}}{\partial \Delta \theta_3} & \frac{\partial \Delta Q_{L2}}{\partial \Delta \theta_4} & \frac{\partial \Delta Q_{L2}}{\partial \Delta |V_2|} |V_0| & \frac{\partial \Delta Q_{L2}}{\partial \Delta |V_3|} |V_0| & \frac{\partial \Delta Q_{L2}}{\partial \Delta V_4} |V_0| & 0 \\ \frac{\partial \Delta Q_{L3}}{\partial \Delta \theta_2} & \frac{\partial \Delta Q_{L3}}{\partial \Delta \theta_3} & \frac{\partial \Delta Q_{L3}}{\partial \Delta \theta_4} & \frac{\partial \Delta Q_{L3}}{\partial \Delta |V_2|} |V_0| & \frac{\partial \Delta Q_{L3}}{\partial \Delta |V_3|} |V_0| & \frac{\partial \Delta Q_{L3}}{\partial \Delta V_4} |V_0| & 0 \\ \frac{\partial \Delta Q_{L4}}{\partial \Delta \theta_2} & \frac{\partial \Delta Q_{L4}}{\partial \Delta \theta_3} & \frac{\partial \Delta Q_{L4}}{\partial \Delta \theta_4} & \frac{\partial \Delta Q_{L4}}{\partial \Delta |V_2|} |V_0| & \frac{\partial \Delta Q_{L4}}{\partial \Delta |V_3|} |V_0| & \frac{\partial \Delta Q_{L4}}{\partial \Delta V_4} |V_0| & 0 \end{bmatrix} = \begin{bmatrix} \Delta \theta_2 \\ \Delta \theta_3 \\ \Delta \theta_4 \\ \frac{\Delta |V_2|}{|V_0|} \\ \frac{\Delta |V_3|}{|V_0|} \\ \frac{\Delta |V_4|}{|V_0|} \\ \Delta \omega \end{bmatrix} \quad (75)$$

e. Step 5: Set the Initial State.

Flat start: $|V_2|=1$ p.u., $|V_3|=1$ p.u., $|V_4|=1$ p.u., $\Theta_2 = \Theta_3 = \Theta_4 = 0$. Stop criterion: $\Delta x \leq 10^{-5}$.

f. Use Matlab to do the iteration. After 5 iterations, the solution reached the stop criterion.

The results are shown in the following Table 2:

Table 2 4-bus System Power Flow Solution

| | P(p.u.) | Q(p.u.) | V (p.u.) | f(Hz) | K | R |
|--------------|----------------|----------------|------------------|--------------|----------|----------|
| Bus 1 | 0.8711 | j 0.1421 | 1 | 59.95 | 30 | 0.033 |
| Bus 2 | 0.3818 | j 0.0382 | 0.9770 | 59.95 | -- | -- |
| Bus 3 | 0.4753 | j 0.0475 | 0.9750 | 59.95 | -- | -- |
| Bus 4 | 0 | 0 | 0.9932 | 59.95 | -- | -- |

5.1.2 PSS/E Dynamic Simulation Solution

By using the dynamic data file (Figure 17) and the power flow converted save case (Figure 18) as an initial state for the dynamic simulation in PSS/E, we can get the dynamic simulation solution shown in the table on page 74.

| Network data | | Dynamics data | | | | | | | | | | | | |
|--------------|----------|---------------|----------|-----------|----------|-----------|-------|------------|------|--------------|-------------|------------------|------------------|----|
| Bus Number | Bus Name | Base kV | Area Num | Area Name | Zone Num | Zone Name | Owner | Owner Name | Code | Voltage (pu) | Angle (deg) | Normal Vmax (pu) | Normal Vmin (pu) | Em |
| 1 | | 0.0 | 1 | | 1 | | 1 | | 2 | 1.0000 | 1.42 | 1.1000 | 0.9000 | |
| 101 | | 0.0 | 1 | | 1 | | 1 | | 1 | 0.9786 | -2.63 | 1.1000 | 0.9000 | |
| 201 | | 0.0 | 1 | | 1 | | 1 | | 1 | 0.9760 | -3.22 | 1.1000 | 0.9000 | |
| 301 | | 0.0 | 1 | | 1 | | 1 | | 2 | 1.0000 | -0.00 | 1.1000 | 0.9000 | |
| * | | | | | | | | | | | | | | |

Figure 17 4-bus System PF Converted Save Case

| Network data | | Dynamics data | | | | | | | | | | | | | |
|--------------|----------|---------------|-------------|-----------|-------------------------------------|------|---------|-------------------------------------|------|------------------|-------------------------------------|------|------------|--------------------------|------|
| Bus Number | Bus Name | Id | Mbase (MVA) | Generator | In Service | Type | Exciter | In Service | Type | Turbine Governor | In Service | Type | Stabilizer | In Service | Type |
| 1 | | 1 | 100.00 | GENROU | <input checked="" type="checkbox"/> | Std | SCRX | <input checked="" type="checkbox"/> | Std | TGOV5 | <input checked="" type="checkbox"/> | Std | None | <input type="checkbox"/> | |
| 301 | | 1 | 100.00 | GENROU | <input checked="" type="checkbox"/> | Std | SCRX | <input checked="" type="checkbox"/> | Std | TGOV5 | <input checked="" type="checkbox"/> | Std | None | <input type="checkbox"/> | |

Figure 18 4-bus System Dynamic Data File

Now use PSS/E to run the dynamic simulation for the same case and verify the power flow solution from PFLTFS method. For the first 30 seconds, the system is under a normal operation. When $t = 30s$, bus-4 shuts down and then run the dynamic simulation to 1200 seconds. After the long term system frequency control action, the system finally settled down when $t = 850s$ with a new system frequency $f = 59.93$ Hz.

Table 3 4-bus System Dynamic Simulation Solution

| | P(p.u.) | Q(p.u.) | V (p.u.) | f(Hz) | K | R |
|--------------|----------------|----------------|------------------|--------------|----------|----------|
| Bus 1 | 0.8852 | j 0.1591 | 0.9904 | 59.93 | 30 | 0.033 |
| Bus 2 | 0.3853 | j 0.0385 | 0.9606 | 59.93 | -- | -- |
| Bus 3 | 0.4810 | j 0.0481 | 0.9574 | 59.93 | -- | -- |
| Bus 4 | 0 | 0 | 0.9767 | 59.93 | -- | -- |

The results from the dynamic simulation in Table 3 are very close to the results calculated from augmented PF equations.

The error between the two system frequencies is 0.03%. It verifies that using augmented PF equations to calculate the system frequency deviation is practical.

Now we are able to use the output channel plots from PSS/E dynamic simulation to analyze the behavior of frequency responses and other variables.

5.1.2.1 Long Term Frequency Response

Using PSS/E to run the dynamic simulation for the same 4-bus system study case, the frequency response can be shown as below. (Figure 19)

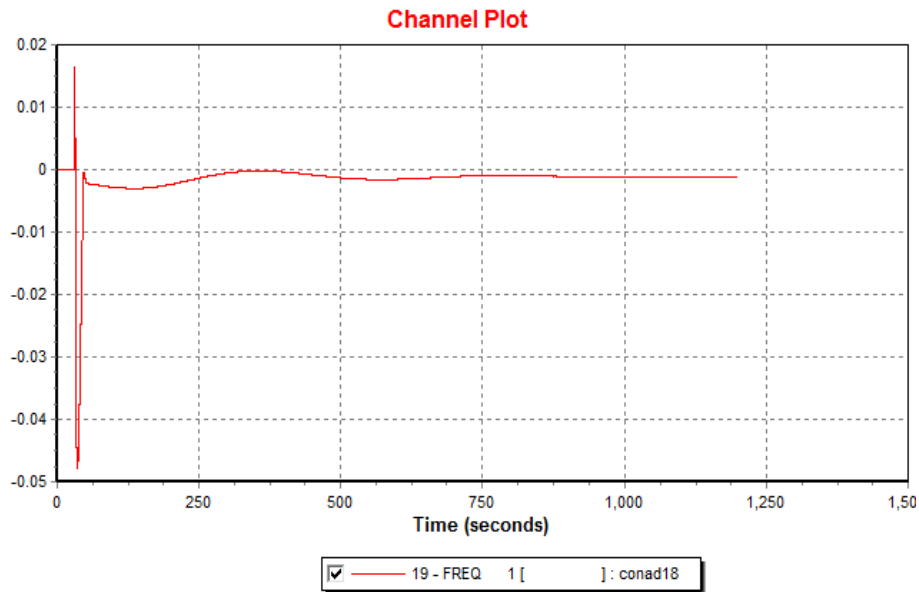


Figure 19 Long-term System Frequency Response

For the first 30 seconds, the system is under a normal operation. When $t = 30s$, bus-4 shuts down. Then run the dynamic simulation to 1200 seconds. The system settled down at $t = 850s$ with a new frequency.

As we discussed in chapter 3, the frequency response can be divided into four stages:

Stage 1: Rotor swings in the generator (first few seconds);

Stage 2: Frequency drop (a few seconds);

Stage 3: Primary control and Secondary control (around 15 minutes);

Stage 4: Settle down (more than 15 minutes).

Figure 20 shows the frequency response of first 120 seconds.

Stage 1 - Rotor Swings

The sudden tripping of bus 4 will produce a large rotor swings at first. That is why there is a large increase in this response from 30s – 30.808s.

Stage 2 - Frequency Drop

The power imbalance and voltage drop will cause the frequency to drop just very few seconds after Stage 1.

Stage 3 – Frequency Control

Stage 3 depends on how the generators and loads react to the frequency drop. As the frequency drops, the turbine governor opens the valve to increase the mechanical power. The relation between increased output and the frequency drop is defined by the droop characteristic K .

At the meantime, the regulator will send the feedback signal to the generators to adjust the setting point. Secondary control tries to bring the frequency deviation to 0.

In this case, the generation doesn't have enough spinning reserve. When the setting point reaches its maximum output, the secondary control will not work and there will be only primary control.

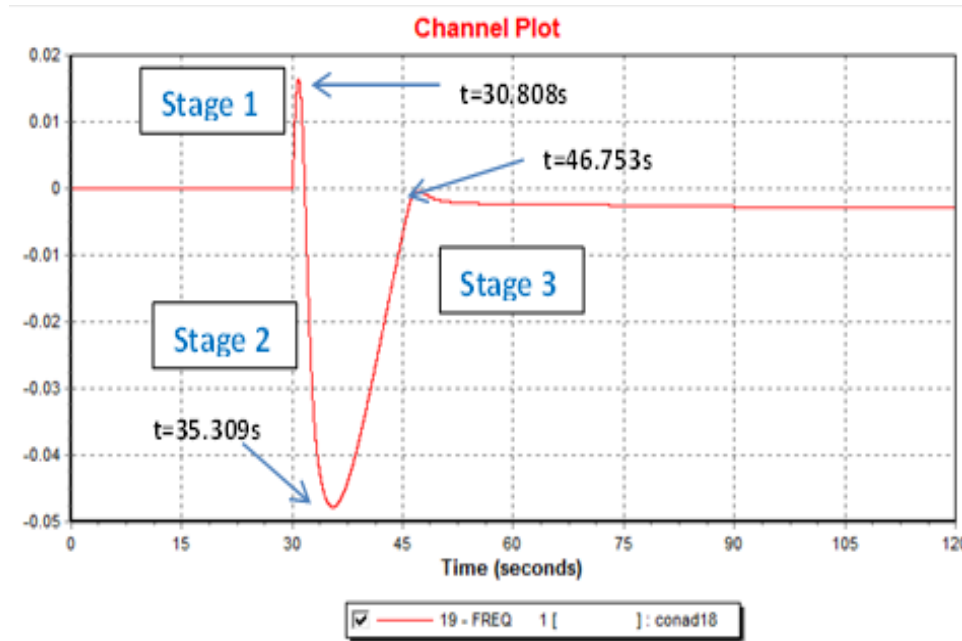


Figure 20 System Frequency Response in First 120s

Stage 4 – Settle down

The system frequency settles down when $t = 850s$. There is only primary control remained, because the reference set point has reached its maximum value and secondary loop control now is saturated. The primary control is usually on a purely local generator level [26].

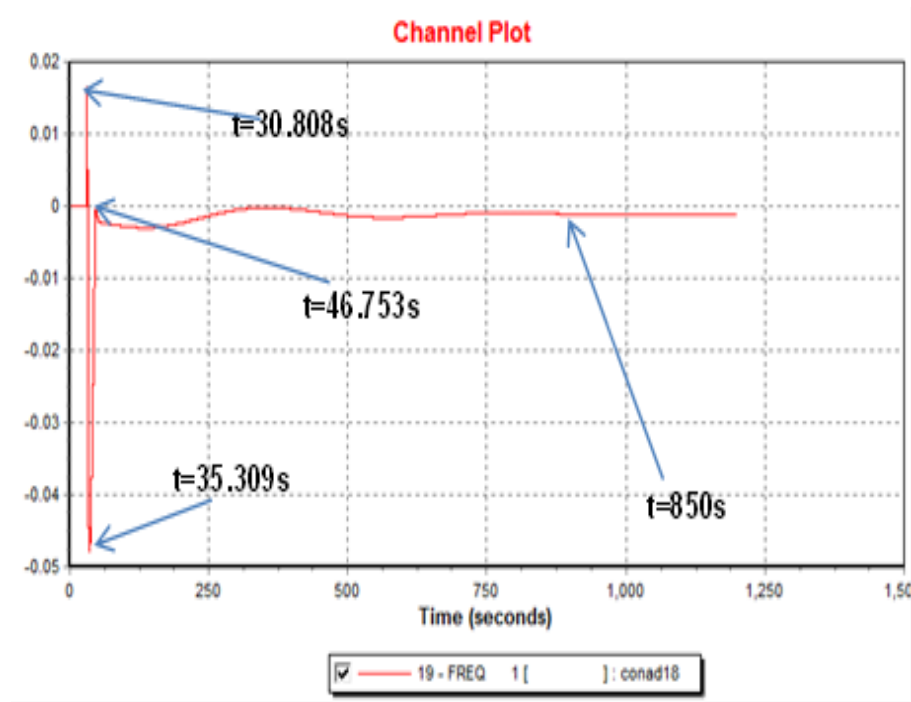


Figure 21 The Long-term System Frequency Response

The system frequency finally settles down when $t = 850s$ (Figure 21) at a frequency = 59.93 Hz. That means the system took about 12 minutes to settle down to a steady state. This result is very close to the frequency calculated from PFLTFS method (59.95 Hz).

The detailed power flow solutions from both the PFLTFS method and the PSS/E dynamic simulation are shown in Table 4.

Table 4 PF Solution with a Constant Impedance Load

| Bus No. | PFLTFS (p.u.) | PSS/E (p.u.) |
|----------------------|----------------------|---------------------|
| Bus 1(output) | 0.8751 + j 0.1422 | 0.8852 + j 0.1591 |
| Bus 2(load) | 0.3836 + j 0.0384 | 0.3853 + j 0.0385 |
| Bus 3(load) | 0.4772 + j 0.0477 | 0.4810 + j 0.0481 |
| Bus 4(load) | 0 + j 0 | 0 + j 0 |
| Line loss | 0.014 | 0.018 |
| Bus 1(volt) | 1.0000 | 0.9904 |
| Bus 2(volt) | 0.9770 | 0.9606 |
| Bus 3(volt) | 0.9750 | 0.9574 |
| Bus 4(volt) | 0.9932 | 0.9767 |
| Bus 2(angle) | -3.480° | -4.210° |
| Bus 3(angle) | -3.680° | -4.421° |
| Bus 4(angle) | -0.650° | -1.440° |
| Frequency | 59.95 Hz | 59.93 Hz |

We can see the two frequencies are very close.

5.1.2.2 Bus Voltage

Figure 22 shows the voltage at bus-1. Bus-1 is a PV bus.

Because of the existence of stabilizer, the voltage will be regulated to its nominal value very quickly.

The left plot of Figure 23 shows the voltage at bus-2. Bus-2 is a PQ bus

The right plot of Figure 23 shows the voltage at bus-23. Bus-3 is also a PQ bus

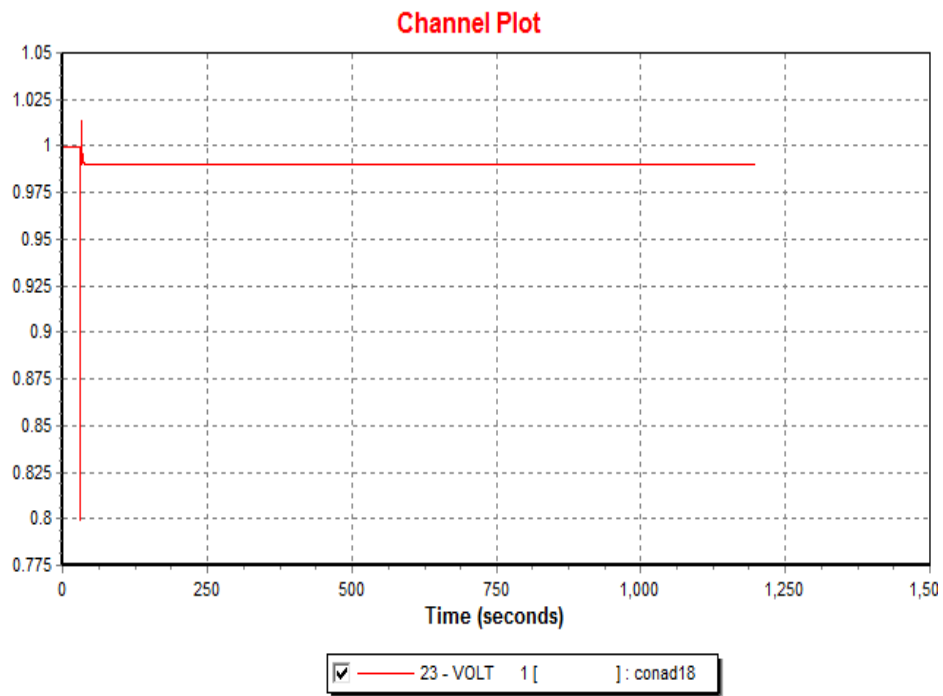


Figure 22 Voltage at Bus-1

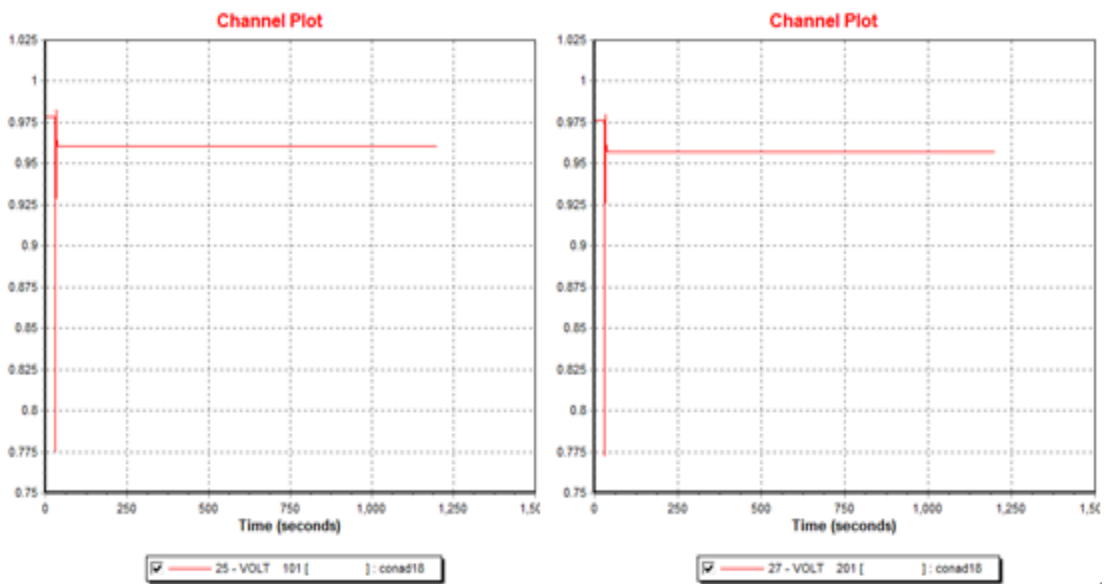


Figure 23 Voltage at Bus-2 and Bus-3

The load voltage changes are exactly the same to the generator voltage changes.

For the generator voltage, from Figure 24 we can see there is a big voltage drop in the system at $t=30s$, because:

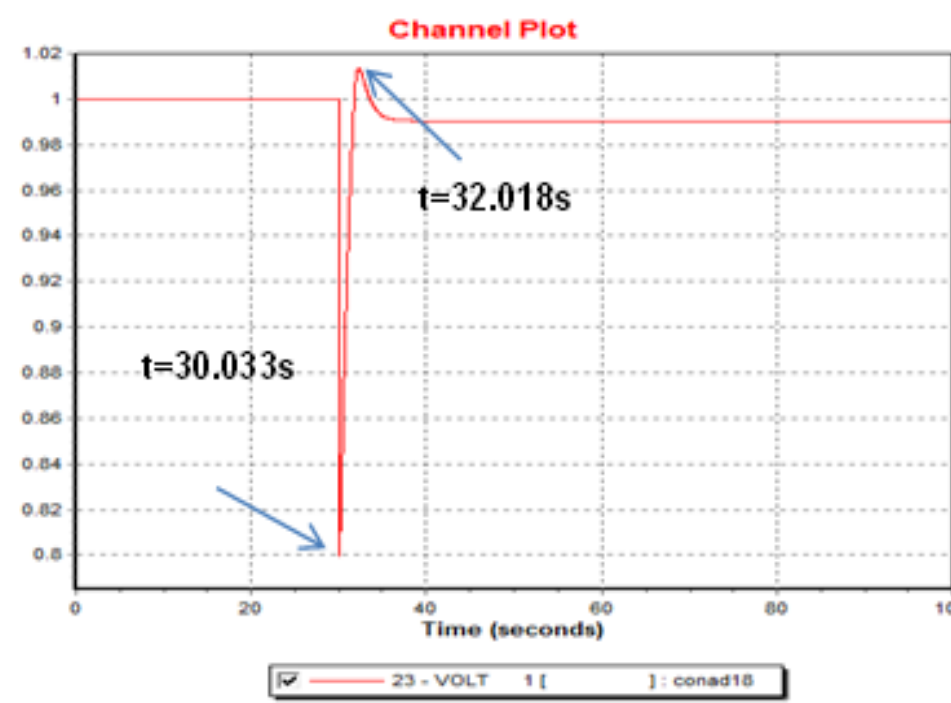


Figure 24 Voltage at Bus-1 in First 120s

The generator tripping in Bus-4 increases the equivalent system reactance.

In addition, the unit tripping reduces the system's capability to generate power. Thus it increases voltage drops in lines and therefore depresses network voltages [27].

On the other hand, the voltage control devices in the system try to bring the voltage back to regulated value 1 p.u .

That is why the voltage increases and goes back to the normal value. But from the figure we can see that, there is a slight difference between the steady state voltage and the normal value.

5.1.2.3 Load Real Power

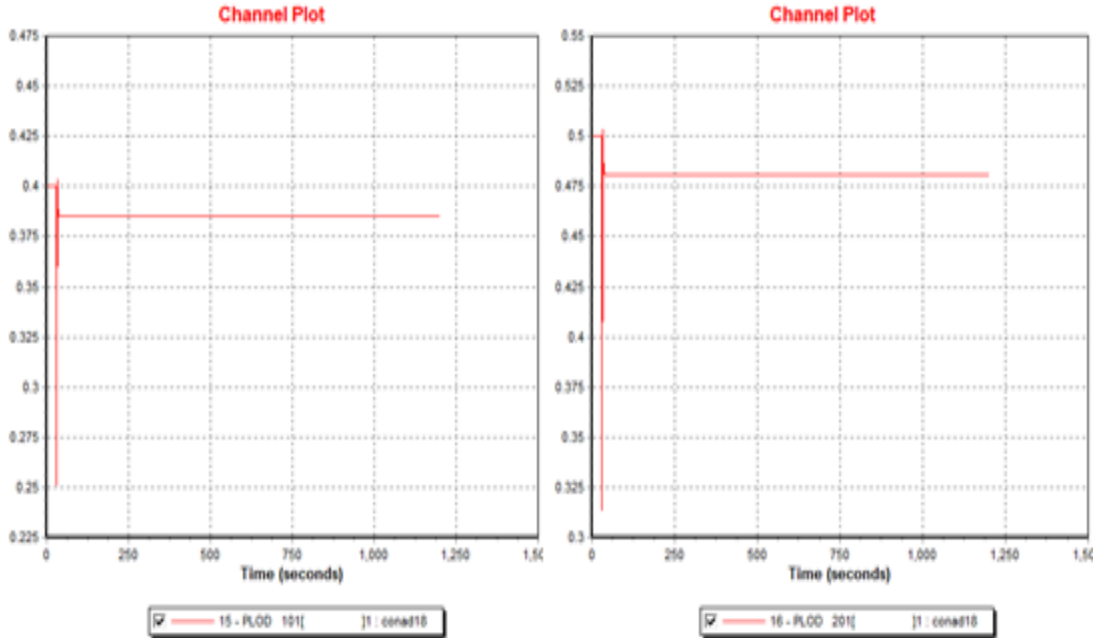


Figure 25 Load at Bus-2 and Bus-3

The above Figure 25 shows the load real power behavior in this dynamic simulation. Compared these two figures to the voltage plots in the system, the trend of load plot is the same to the voltage plot's trend, because the load model is constant impedance and the load power changes proportionally to the voltage squared.

5.1.2.4 Generator Output

For the generator power output, Figure 26 shows the entire plot of electrical power and mechanical power at bus-1 in the system for 1200s, while Figure 27 gives a more detailed plot for the first 120s.

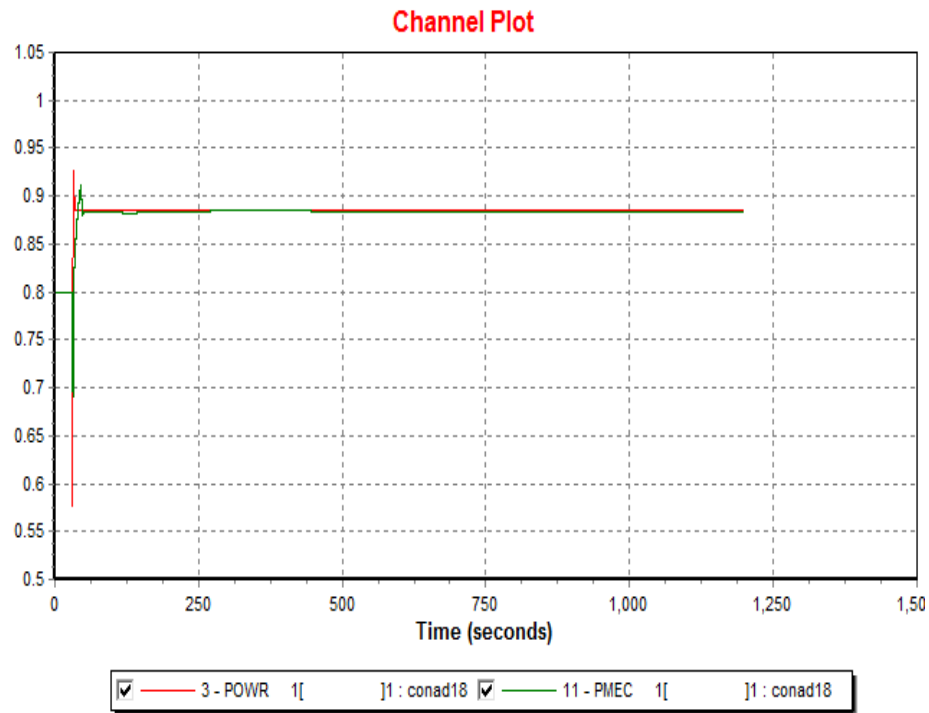


Figure 26 The Generator Output Power and Mechanical Power at Bus-1

In Figure 26, the red trajectory is the electrical power and the green trajectory is the mechanical power.

For electrical power, it goes down very fast, because the voltage at bus-1 rapidly decreased at first.

The electrical power reaches its minimum value when $t = 30.033s$, which is the same time when the voltage reaches the bottom. Later with the regulator and other voltage control devices, the voltage goes back later, thus electrical power also increases.

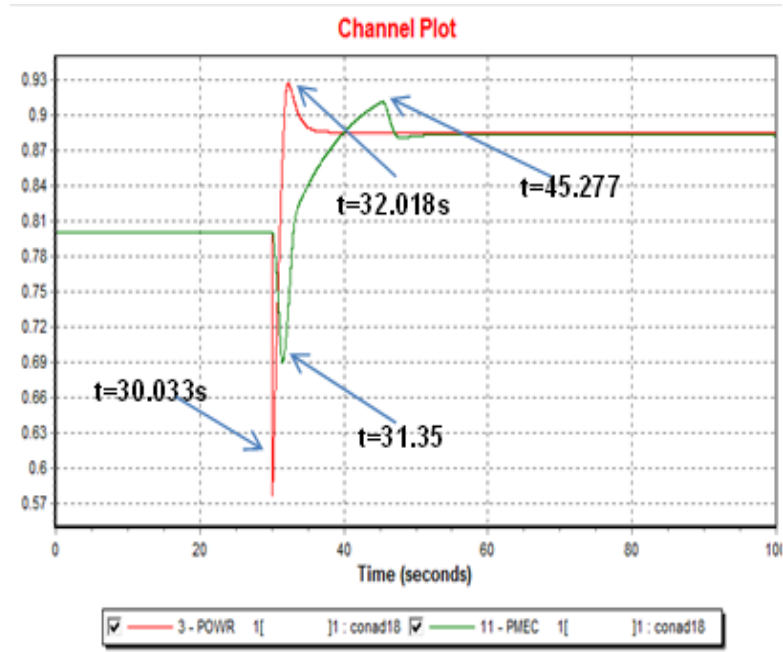


Figure 27 P_{elec} and P_{mech} at Bus-1 in First 120s

For mechanical power, because a large rotor swings occurs and the frequency increases rapidly, the mechanical power goes down very fast at first. (Figure 27) The mechanical power reaches its minimum value when $t = 31.35s$. After the primary control and secondary control starts to work, the mechanical power also begins to increase. When the I – controller is saturated, only primary control is activated and the mechanical power reaches its maximum value at the same period.

5.1.2.5 Voltage Angle

From Table 4 we can see that, the voltage angle errors between PFLTFS and PSS/E dynamic simulation are within 0.8° , which seem to be large errors. However, in practice, only the line flow matters, and since line flows only depends on angle differences among buses, which has much smaller errors.

We demonstrate by taking the worst case as an example:

The bus 2 angle error between PFLTFS and PSS/E is 0.79° . This is the biggest angle error in the results. If we use the PSS/E bus 2 voltage angle as a base value, the error percentage is 18.5%.

Now let's calculate the line flow on Branch 1-2:

In PFLTFS, the line flow is shown in Equation (76):

$$I_{PFLTFS12} = (|V_2| \angle \theta_2 - |V_1| \angle \theta_1) / Z_{12} = (-0.34 + j0.047) p.u. \quad (76)$$

In PSS/E, the line flow is shown in Equation (77):

$$I_{PSS/E12} = (|V_2| \angle \theta_2 - |V_1| \angle \theta_1) / Z_{12} = (-0.36 + j0.071) p.u. \quad (77)$$

The line flow difference between PFLTFS and PSS/E is $(0.02-j0.03)$ p.u.. Take the PSS/E line flow magnitude as the base value; the error percentage is 5%. Compared to angle θ_2 error 18.5%, the line flow error 5% is much smaller. This can be explained as follows:

1. The voltage angle differences are used to calculate the line flow. For example, the angle difference θ_{23} in PFLTFS is 0.2° while the angle difference θ_{23} in PSS/E is 0.211° . The angle difference error is 0.011° . Take the angle difference θ_{23} in PSS/E as the base value; the angle difference error percentage is 5.2%.

2. In addition, after we calculate $\sin\theta_{ij}$ and $\cos\theta_{ij}$, the error will be even smaller.

One possible cause of big voltage angle errors might be the integration in the dynamic simulation. In PFLTFS, the slack bus reference angle is fixed to 0° . However, in PSS/E, the slack bus reference angle and all other bus angles keep going down because of the lack of an angle reference. This will lead to errors in the integration and in thus the bus voltage angles.

5.1.3 4-bus System with a Different Load Model

In section 5.1.1 and 5.1.2, we use the PFLTFS method and the PSS/E dynamic simulation to run a small 4-bus system study case with a constant impedance model. The PSS/E

results are very close to the novel static power flow solution. Now we will consider the same 4-bus system study case but with a different load model.

According to chapter 2, the ZIP model is the combination of these three models. Equation (4) and Equation (5) represent the ZIP model in a polynomial form:

$$P_{Li} = P_{Loi} \left[a_1 \left(\frac{|V_i|}{|V_0|} \right)^2 + a_2 \left(\frac{|V_i|}{|V_0|} \right) + a_3 \right] \quad (37)$$

$$Q_{Li} = Q_{Loi} \left[a_1 \left(\frac{|V_i|}{|V_0|} \right)^2 + a_2 \left(\frac{|V_i|}{|V_0|} \right) + a_3 \right] \quad (38)$$

$$a_1 + a_2 + a_3 = 1 \quad (39)$$

In this section, the load model will be a combination of constant current model and constant impedance model.

$$P_{Li} = P_{Loi} \left[0.7 * \left(\frac{|V_i|}{|V_0|} \right)^2 + 0.3 * \left(\frac{|V_i|}{|V_0|} \right) \right] \quad (78)$$

$$Q_{Li} = Q_{Loi} \left[0.7 * \left(\frac{|V_i|}{|V_0|} \right)^2 + 0.3 * \left(\frac{|V_i|}{|V_0|} \right) \right] \quad (79)$$

From Equation (78) and Equation (79), the load model in this case consists of 70% constant impedance model and 30% constant current model.

For the static power flow solution, the system new frequency settles down at $f = 59.95$ Hz. For PSS/E dynamic simulation, in the first 30 seconds, the system is under a normal operation.

When $t = 30s$, bus-4 generator trips and then run the dynamic simulation to 1200 seconds. The angle error is within 0.4%. After the system frequency control action, the system finally settled down when $t = 850s$ with a new system frequency $f = 59.92$ Hz. The error between two frequencies is 0.05%.

The detailed power flow solutions from both the PFLTFS method and the PSS/E dynamic simulation are shown in Table 5.

Table 5 PF Solution with a Mixed Load

| Bus No. | PFLTFS(p.u.) | PSS/E(p.u.) |
|----------------------|--------------------------|--------------------------|
| Bus 1(output) | 0.8737 + j 0.1432 | 0.8899 + j 0.1604 |
| Bus 2(load) | 0.3845 + j 0.0384 | 0.3873 + j 0.0387 |
| Bus 3(load) | 0.4752 + j 0.0479 | 0.4836 + j 0.0484 |
| Bus 4(load) | 0 + j 0 | 0 + j 0 |
| Line loss | 0.014 | 0.019 |
| Bus 1(volt) | 1.0000 | 0.9903 |
| Bus 2(volt) | 0.9769 | 0.9603 |
| Bus 3(volt) | 0.9748 | 0.9570 |
| Bus 4(volt) | 0.9932 | 0.9765 |
| Bus 2(angle) | -3.42° | -4.29° |
| Bus 3(angle) | -3.69° | -4.67° |
| Bus 4(angle) | -0.65° | -1.44° |
| Frequency | 59.95 Hz | 59.92 Hz |

5.2 IEEE 118-bus System Scenarios

Now the PFLTFS should be expanded to a large system, for example the IEEE 118- bus system. In this section, the method will be applied in several different scenarios and then compared to the simulation results from PSS/E.

The IEEE 118-bus system scheme is given below in Figure 28. This system represents a portion of American Electric Power System in the Midwestern US area as of December, 1962. The data is made available to the electricity utility industry as a standard test case.

In this system, the bus-69 is the slack bus and the 118-bus system has 54 PV buses in total. The total real power output is 4375 MWA.

Output > 100 MW: 12 buses (10; 25; 26; 49; 59; 61; 65; 66; 69; 80; 89; 100.)

Output < 100 MW: 7 buses (12; 31; 46; 54; 87; 103; 111.)

Output = 0 MW: 35 buses

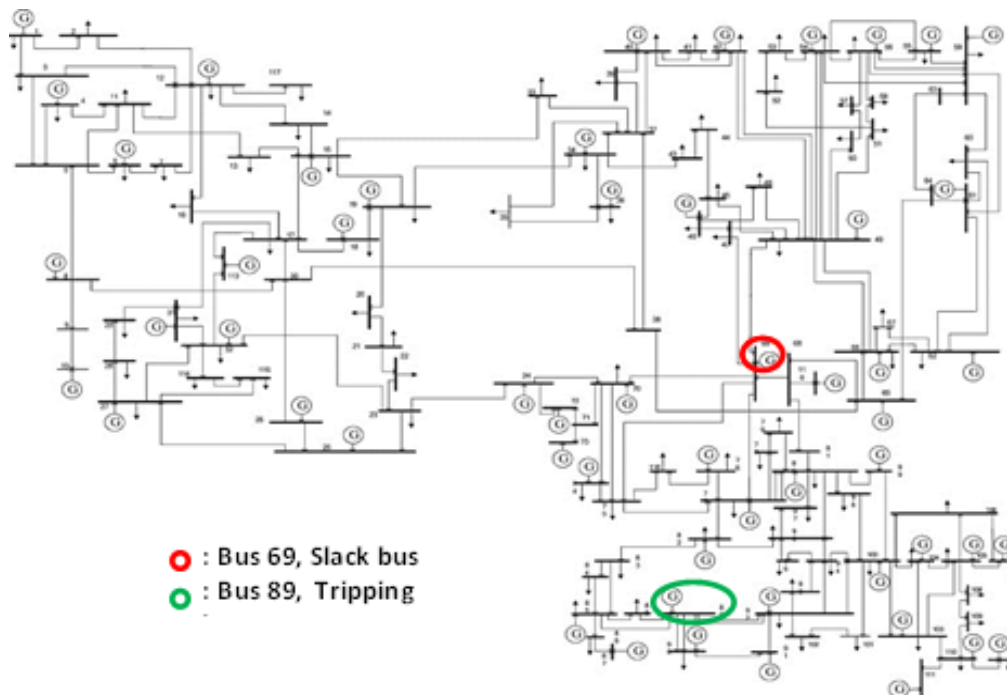


Figure 28 IEEE 118-bus System

The assumptions are:

- a. All the values are uniformed (the Base MWA is 100 MWA; the Base Frequency is 60 Hz).
- b. The droop $1/R = K = 50$.
- c. The load is not frequency dependent.

Scenarios

To better study the PFLTFS method in a large system, several scenarios will be used here:

Scenario 1: Trip 14% output when all the generators are at their maximum output (0% reserve, no secondary loop). The load model is constant impedance.

Scenario 2: Trip 14% output when the system has 8% output reserve (including secondary loop). The load model is constant impedance.

Scenario 3: Trip 14% output when all the generators are at their maximum output (0% reserve, no secondary loop). The load model consists of 30% constant current and 70% constant impedance.

Scenario 4: Trip 14% output when the system has 8% output reserve (includes secondary loop). The load model consists of 30% constant current and 70% constant impedance.

Scenario 5: Severe cases when frequency drops to 58 Hz.

5.2.1 Scenario 1

Trip 14% output when all the generators are at their maximum output (0% reserve, no secondary loop). The load model is constant impedance.

Figure 29 and Figure 30 are the snapshots of the power flow save case and the dynamic data file that are used for the IEEE 118-bus system dynamic simulation.

| Bus Number | Bus Name | Base kV | Area Num | Area Name | Zone Num | Zone Name | Owner | Owner Name | Code | Voltage (pu) | Angle (deg) | Normal Vmax (pu) | Normal Vmin (pu) |
|------------|----------|---------|----------|-----------|----------|-----------|-------|------------|------|--------------|-------------|------------------|------------------|
| 1 | BUS-1 | 100.0 | 1 | | 1 | | 1 | | 2 | 0.9550 | -20.82 | 1.1000 | 0.9000 |
| 2 | BUS-2 | 100.0 | 1 | | 1 | | 1 | | 1 | 0.9714 | -20.28 | 1.1000 | 0.9000 |
| 3 | BUS-3 | 100.0 | 1 | | 1 | | 1 | | 1 | 0.9677 | -19.93 | 1.1000 | 0.9000 |
| 4 | BUS-4 | 100.0 | 1 | | 1 | | 1 | | 2 | 0.9980 | -16.21 | 1.1000 | 0.9000 |
| 5 | BUS-5 | 100.0 | 1 | | 1 | | 1 | | 1 | 1.0020 | -15.76 | 1.1000 | 0.9000 |
| 6 | BUS-6 | 100.0 | 1 | | 1 | | 1 | | 2 | 0.9900 | -18.50 | 1.1000 | 0.9000 |
| 7 | BUS-7 | 100.0 | 1 | | 1 | | 1 | | 1 | 0.9893 | -18.94 | 1.1000 | 0.9000 |
| 8 | BUS-8 | 100.0 | 1 | | 1 | | 1 | | 2 | 1.0150 | -10.73 | 1.1000 | 0.9000 |
| 9 | BUS-9 | 100.0 | 1 | | 1 | | 1 | | 1 | 1.0262 | -3.28 | 1.1000 | 0.9000 |
| 10 | BUS-10 | 100.0 | 1 | | 1 | | 1 | | 2 | 1.0500 | 4.35 | 1.1000 | 0.9000 |
| 11 | BUS-11 | 100.0 | 1 | | 1 | | 1 | | 1 | 0.9851 | -18.79 | 1.1000 | 0.9000 |
| 12 | BUS-12 | 100.0 | 1 | | 1 | | 1 | | 2 | 0.9900 | -19.31 | 1.1000 | 0.9000 |
| 13 | BUS-13 | 100.0 | 1 | | 1 | | 1 | | 1 | 0.9683 | -20.18 | 1.1000 | 0.9000 |
| 14 | BUS-14 | 100.0 | 1 | | 1 | | 1 | | 1 | 0.9836 | -20.04 | 1.1000 | 0.9000 |
| 15 | BUS-15 | 100.0 | 1 | | 1 | | 1 | | 2 | 0.9700 | -20.39 | 1.1000 | 0.9000 |
| 16 | BUS-16 | 100.0 | 1 | | 1 | | 1 | | 1 | 0.9838 | -19.60 | 1.1000 | 0.9000 |
| 17 | BUS-17 | 100.0 | 1 | | 1 | | 1 | | 1 | 0.9949 | -17.79 | 1.1000 | 0.9000 |
| 18 | BUS-18 | 100.0 | 1 | | 1 | | 1 | | 2 | 0.9730 | -20.05 | 1.1000 | 0.9000 |
| 19 | BUS-19 | 100.0 | 1 | | 1 | | 1 | | 2 | 0.9634 | -20.59 | 1.1000 | 0.9000 |
| 20 | BUS-20 | 100.0 | 1 | | 1 | | 1 | | 1 | 0.9577 | -19.59 | 1.1000 | 0.9000 |
| 21 | BUS-21 | 100.0 | 1 | | 1 | | 1 | | 1 | 0.9582 | -17.91 | 1.1000 | 0.9000 |
| 22 | BUS-22 | 100.0 | 1 | | 1 | | 1 | | 1 | 0.9692 | -15.26 | 1.1000 | 0.9000 |
| 23 | BUS-23 | 100.0 | 1 | | 1 | | 1 | | 1 | 0.9995 | -10.18 | 1.1000 | 0.9000 |
| 24 | BUS-24 | 100.0 | 1 | | 1 | | 1 | | 2 | 0.9920 | -10.11 | 1.1000 | 0.9000 |
| 25 | BUS-25 | 100.0 | 1 | | 1 | | 1 | | 2 | 1.0500 | -3.38 | 1.1000 | 0.9000 |
| 26 | BUS-26 | 100.0 | 1 | | 1 | | 1 | | 2 | 1.0150 | -1.85 | 1.1000 | 0.9000 |

Figure 29 IEEE 118-bus System PF Save Case

| Bus Number | Bus Name | Id | Mbase (MVA) | Generator | In Service | Type | Exciter | In Service | Type | Turbine Governor | In Service | Type | Stabilizer | In Service | Type |
|------------|----------|----|-------------|-----------|-------------------------------------|------|---------|-------------------------------------|------|------------------|-------------------------------------|------|------------|-------------------------------------|------|
| 10 | BUS-10 | 1 | 1000.00 | GENROU | <input checked="" type="checkbox"/> | Stnd | EEET2 | <input checked="" type="checkbox"/> | Stnd | TGOV5 | <input checked="" type="checkbox"/> | Stnd | EEEEST | <input checked="" type="checkbox"/> | Stn |
| 25 | BUS-25 | 1 | 1000.00 | GENROU | <input checked="" type="checkbox"/> | Stnd | EEET2 | <input checked="" type="checkbox"/> | Stnd | TGOV5 | <input checked="" type="checkbox"/> | Stnd | EEEEST | <input checked="" type="checkbox"/> | Stn |
| 26 | BUS-26 | 1 | 1000.00 | GENROU | <input checked="" type="checkbox"/> | Stnd | EEET2 | <input checked="" type="checkbox"/> | Stnd | TGOV5 | <input checked="" type="checkbox"/> | Stnd | EEEEST | <input checked="" type="checkbox"/> | Stn |
| 49 | BUS-49 | 1 | 1000.00 | GENROU | <input checked="" type="checkbox"/> | Stnd | EEET2 | <input checked="" type="checkbox"/> | Stnd | TGOV5 | <input checked="" type="checkbox"/> | Stnd | EEEEST | <input checked="" type="checkbox"/> | Stn |
| 59 | BUS-59 | 1 | 1000.00 | GENROU | <input checked="" type="checkbox"/> | Stnd | EEET2 | <input checked="" type="checkbox"/> | Stnd | TGOV5 | <input checked="" type="checkbox"/> | Stnd | EEEEST | <input checked="" type="checkbox"/> | Stn |
| 61 | BUS-61 | 1 | 1000.00 | GENROU | <input checked="" type="checkbox"/> | Stnd | EEET2 | <input checked="" type="checkbox"/> | Stnd | TGOV5 | <input checked="" type="checkbox"/> | Stnd | EEEEST | <input checked="" type="checkbox"/> | Stn |
| 65 | BUS-65 | 1 | 1000.00 | GENROU | <input checked="" type="checkbox"/> | Stnd | EEET2 | <input checked="" type="checkbox"/> | Stnd | TGOV5 | <input checked="" type="checkbox"/> | Stnd | EEEEST | <input checked="" type="checkbox"/> | Stn |
| 66 | BUS-66 | 1 | 1000.00 | GENROU | <input checked="" type="checkbox"/> | Stnd | EEET2 | <input checked="" type="checkbox"/> | Stnd | TGOV5 | <input checked="" type="checkbox"/> | Stnd | EEEEST | <input checked="" type="checkbox"/> | Stn |
| 69 | BUS-69 | 1 | 1000.00 | GENROU | <input checked="" type="checkbox"/> | Stnd | EEET2 | <input checked="" type="checkbox"/> | Stnd | TGOV5 | <input checked="" type="checkbox"/> | Stnd | EEEEST | <input checked="" type="checkbox"/> | Stn |
| 80 | BUS-80 | 1 | 1000.00 | GENROU | <input checked="" type="checkbox"/> | Stnd | EEET2 | <input checked="" type="checkbox"/> | Stnd | TGOV5 | <input checked="" type="checkbox"/> | Stnd | EEEEST | <input checked="" type="checkbox"/> | Stn |
| 89 | BUS-89 | 1 | 1000.00 | GENROU | <input checked="" type="checkbox"/> | Stnd | EEET2 | <input checked="" type="checkbox"/> | Stnd | TGOV5 | <input checked="" type="checkbox"/> | Stnd | EEEEST | <input checked="" type="checkbox"/> | Stn |
| 100 | BUS-100 | 1 | 1000.00 | GENROU | <input checked="" type="checkbox"/> | Stnd | EEET2 | <input checked="" type="checkbox"/> | Stnd | TGOV5 | <input checked="" type="checkbox"/> | Stnd | EEEEST | <input checked="" type="checkbox"/> | Stn |
| 12 | BUS-12 | 1 | 100.00 | GENROU | <input checked="" type="checkbox"/> | Stnd | SEXS | <input checked="" type="checkbox"/> | Stnd | TGOV1 | <input checked="" type="checkbox"/> | Stnd | None | <input type="checkbox"/> | |
| 31 | BUS-31 | 1 | 100.00 | GENROU | <input checked="" type="checkbox"/> | Stnd | SEXS | <input checked="" type="checkbox"/> | Stnd | TGOV1 | <input checked="" type="checkbox"/> | Stnd | None | <input type="checkbox"/> | |
| 46 | BUS-46 | 1 | 100.00 | GENROU | <input checked="" type="checkbox"/> | Stnd | SEXS | <input checked="" type="checkbox"/> | Stnd | TGOV1 | <input checked="" type="checkbox"/> | Stnd | None | <input type="checkbox"/> | |
| 54 | BUS-54 | 1 | 100.00 | GENROU | <input checked="" type="checkbox"/> | Stnd | SEXS | <input checked="" type="checkbox"/> | Stnd | TGOV1 | <input checked="" type="checkbox"/> | Stnd | None | <input type="checkbox"/> | |
| 87 | BUS-87 | 1 | 100.00 | GENROU | <input checked="" type="checkbox"/> | Stnd | SEXS | <input checked="" type="checkbox"/> | Stnd | TGOV1 | <input checked="" type="checkbox"/> | Stnd | None | <input type="checkbox"/> | |
| 103 | BUS-103 | 1 | 100.00 | GENROU | <input checked="" type="checkbox"/> | Stnd | SEXS | <input checked="" type="checkbox"/> | Stnd | TGOV1 | <input checked="" type="checkbox"/> | Stnd | None | <input type="checkbox"/> | |
| 111 | BUS-111 | 1 | 100.00 | GENROU | <input checked="" type="checkbox"/> | Stnd | SEXS | <input checked="" type="checkbox"/> | Stnd | TGOV1 | <input checked="" type="checkbox"/> | Stnd | None | <input type="checkbox"/> | |
| 1 | BUS-1 | 1 | 100.00 | GENROU | <input checked="" type="checkbox"/> | Stnd | SEXS | <input checked="" type="checkbox"/> | Stnd | None | <input type="checkbox"/> | Stnd | None | <input type="checkbox"/> | |
| 4 | BUS-4 | 1 | 100.00 | GENROU | <input checked="" type="checkbox"/> | Stnd | SEXS | <input checked="" type="checkbox"/> | Stnd | None | <input type="checkbox"/> | Stnd | None | <input type="checkbox"/> | |
| 6 | BUS-6 | 1 | 100.00 | GENROU | <input checked="" type="checkbox"/> | Stnd | SEXS | <input checked="" type="checkbox"/> | Stnd | None | <input type="checkbox"/> | Stnd | None | <input type="checkbox"/> | |
| 8 | BUS-8 | 1 | 100.00 | GENROU | <input checked="" type="checkbox"/> | Stnd | SEXS | <input checked="" type="checkbox"/> | Stnd | None | <input type="checkbox"/> | Stnd | None | <input type="checkbox"/> | |
| 15 | BUS-15 | 1 | 100.00 | GENROU | <input checked="" type="checkbox"/> | Stnd | SEXS | <input checked="" type="checkbox"/> | Stnd | None | <input type="checkbox"/> | Stnd | None | <input type="checkbox"/> | |
| 18 | BUS-18 | 1 | 100.00 | GENROU | <input checked="" type="checkbox"/> | Stnd | SEXS | <input checked="" type="checkbox"/> | Stnd | None | <input type="checkbox"/> | Stnd | None | <input type="checkbox"/> | |

Figure 30 IEEE 118-bus Dynamic Data

In this case, all the generators have hit the limits and there is no spinning reserve. We will trip the generator connected to bus-89. The real power output at bus-89 is 607 MWA, which is 14% of the total output. Assume that the generator of bus-89 suddenly shuts down, try to incorporate the frequency deviation into power flow analysis, and then find the final solution.

Here we just randomly pick bus 10, bus 80 and bus 89 and the results of these three buses are shown below in Table 6.

Table 6 Results Compared Scenario 1

| Bus No. | PFLTFS | PSS/E |
|-------------------|---------------|--------------|
| 10(volt) | 1.05 | 1.05 |
| 10(output) | 4.59 | 4.45 |
| 80(volt) | 1.04 | 1.03 |
| 80(output) | 4.86 | 5.36 |
| 80(load) | 1.40 | 1.29 |
| 89(volt) | 0.99 | 0.99 |
| 89(output) | 0 | 0 |
| 80(angle) | -1.55° | -2.28° |
| 10(angle) | 6.17° | 5.59° |
| Frequency | 59.89 Hz | 59.92 Hz |

The error between two frequencies is 0.05% and the system in the dynamic simulation settled down at $t = 927s$.

The angle error at bus 80 between PFLTFS and PSS/E is 0.73° , and the angle error at bus 10 between PFLTFS and PSS/E is 0.64° . If we use the PSS/E bus angle as the base value, the

error percentage of bus 80 is 32%, and the error percentage of bus 10 is 10%. The angle errors seem big.

However, if we calculate the angle difference, the error will be much smaller as discussed in the earlier example. In PFLTFS, the angle difference between bus 80 and bus 10 is 7.72° ; while in PSS/E the angle difference between bus 80 and bus 10 is 7.87° . The angle difference error between PFLTFS and PSS/E is 0.15° . If we use the angle difference in PSS/E as the base value, the angle difference error percentage would be 2%. As in 4-bus system, the error becomes much smaller. Thus the line flow errors will still be much smaller.

5.2.1.1 Frequency Response

For PSS/E dynamic simulation, in the first 30 seconds, the system is under a normal operation. When $t = 30s$, bus-89 generator trips and then run the dynamic simulation to 1200 seconds.

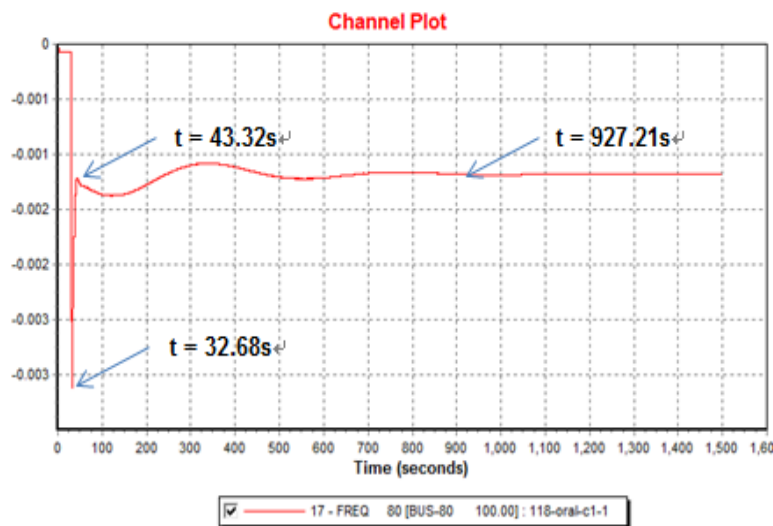


Figure 31 Long-term System Frequency Response

The system settled down at $t = 927.21s$ with a new frequency $f = 59.92Hz$. (Figure 31)

Now we will analyze the frequency response in first 120s (Figure 32):

Stage 1: Because “the sudden disconnection of one of the generators will initially produce large rotor swings in the remaining generating unit and much smaller rotor swings in the other generators within the system” [3], the rotor swings becomes much smaller at bus 80.

That is why the frequency goes down rapidly at first.

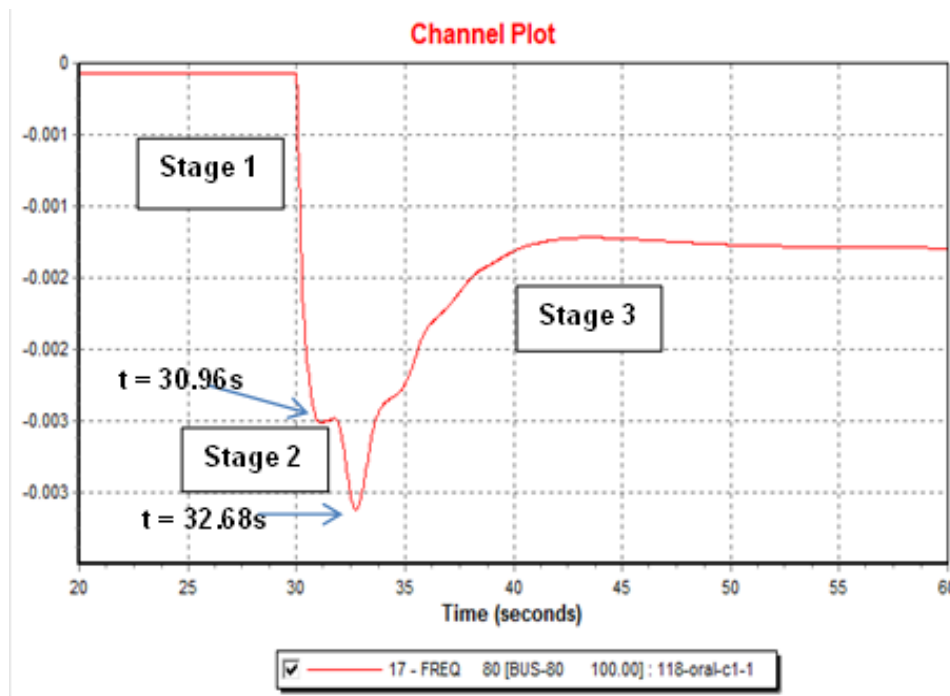


Figure 32 Frequency Response from 20s-60s

Stage 2: The power imbalance and voltage drop will cause the frequency to keep dropping just very few seconds after Stage 1.

Stage 3: Both primary loop control and secondary loop control exist.

In this case, since the spinning reserve is 0%, there is no secondary control.

Stage 4: The system settled down and only the frequency deviation exists.

5.2.1.2 Mechanical Power and Electrical Power at Bus-80

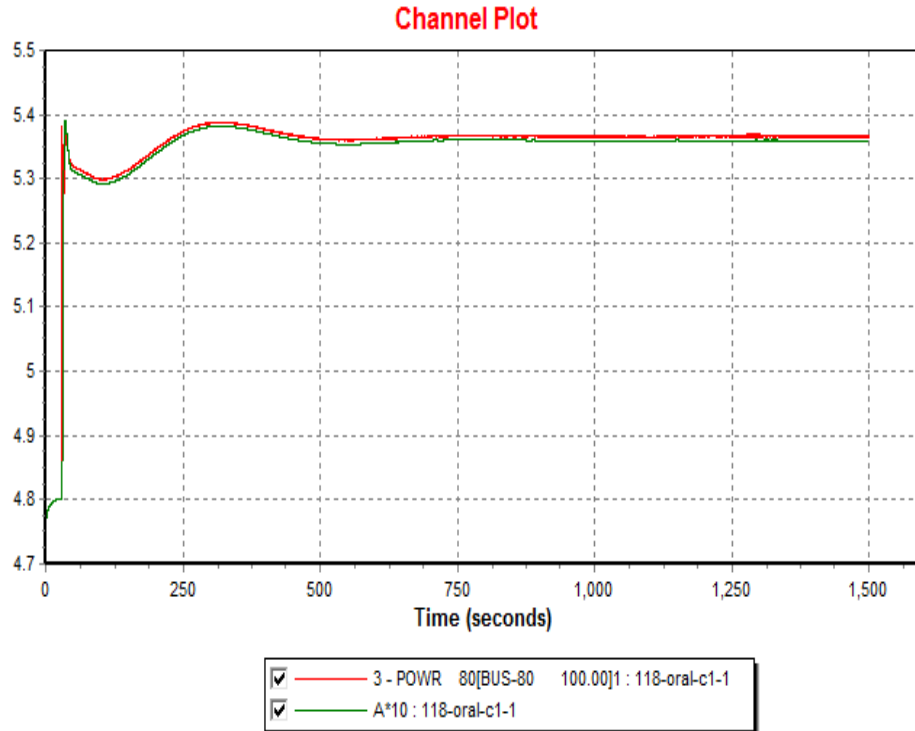


Figure 33 P_{mech} and P_{elec} at Bus-80

The mechanical power and electrical power at bus-80 are shown in Figure 33. This plot shows the general behaviors of the mechanical power and electrical power at PV bus in this 118-bus system.

The red trajectory is the electrical power, and the green trajectory is the mechanical power. Because of the small rotor swings, the frequency decreases at first; thus the mechanical power goes up very fast. Later when the primary control and secondary control start to work, the mechanical power keeps increasing.

Voltage and load at bus-80

Figure 34 shows the voltage change and load change at Bus-80.

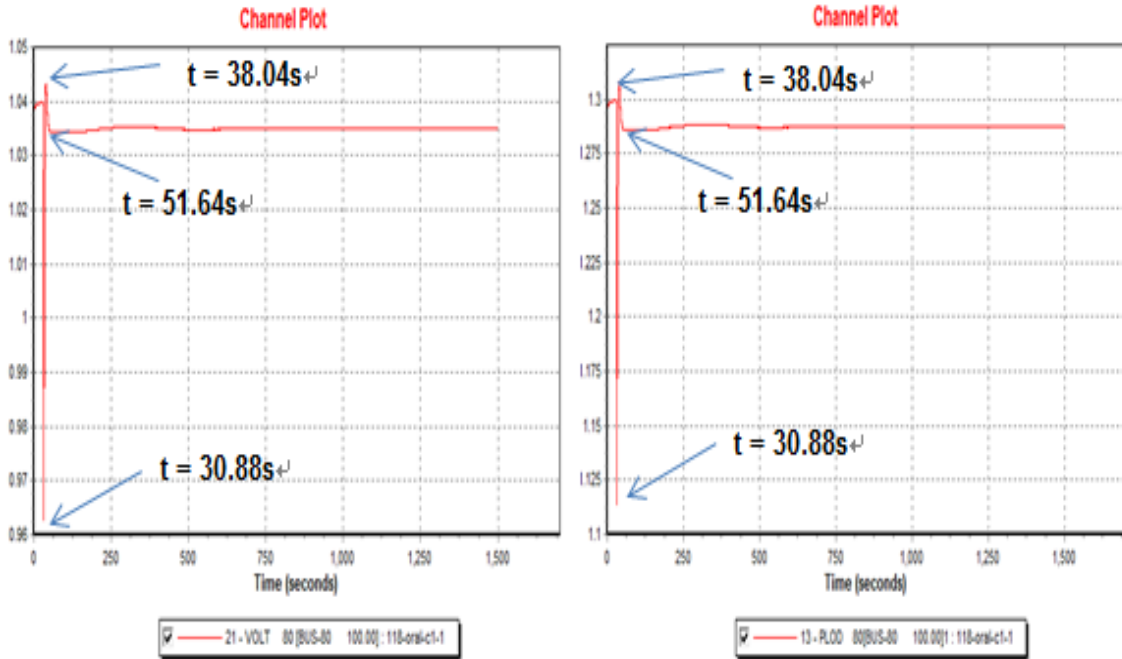


Figure 34 Voltage and Load at Bus-80

Since the load model in this scenario is constant impedance, the load power changes proportionally to the voltage squared [21].

5.2.2 Scenario 2

Trip 14% output when the system has 8% reserve (has secondary loop). The load model is constant impedance.

In this case, the generators haven't hit the limits and there is 8% spinning reserve. Here we just randomly pick bus 10, bus 80 and bus 89 and the results of these three buses are shown below in Table 7.

Table 7 Results Compared in Scenario 2

| Bus No. | PFLTFS | PSS/E |
|------------|----------|----------|
| 10(volt) | 1.05 | 1.05 |
| 10(output) | 4.90 | 4.57 |
| 80(volt) | 1.04 | 1.04 |
| 80(output) | 5.19 | 5.16 |
| 80(load) | 1.41 | 1.29 |
| 89(volt) | 0.99 | 0.99 |
| 89(output) | 0 | 0 |
| Frequency | 59.95 Hz | 59.95 Hz |

The error between two frequencies is 0%. The system settled down at $t = 983s$ with a new system frequency $f = 59.95$ Hz.

5.2.2.1 Frequency Responses in Scenario 1 and 2

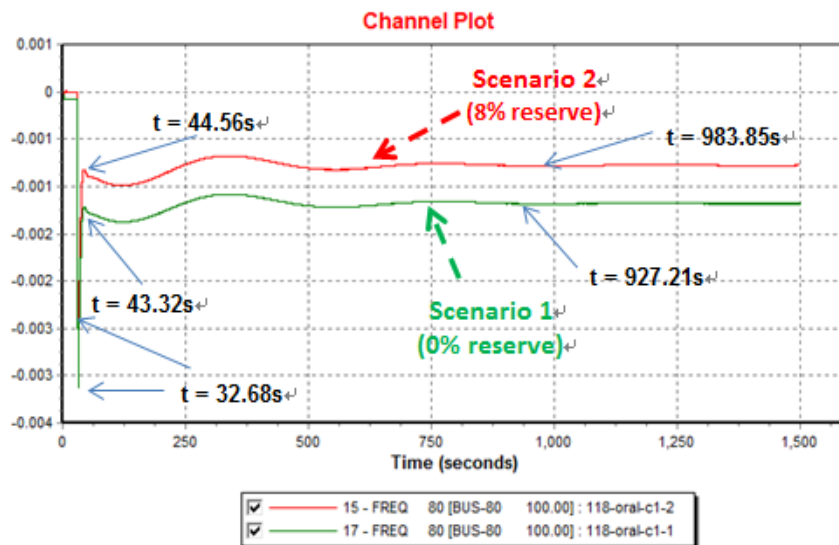


Figure 35 Frequency Responses in Scenario 1 and 2

The only difference between scenario 1 and scenario 2 is there is a 8% spinning reserve in the system in scenario 2. So in scenario 2 the secondary loop control exists and it will take the system longer to settle down. (Figure 35)

In Figure 35, we compared the frequency responses in scenario 1 and scenario 2. Since there is 8% reserve in the system, the secondary loop control exists in scenario 2. It takes longer time than that takes in scenario 1 for the system to settle down to a new frequency. The system finally settled down at $t = 983s$ with a new frequency $f = 59.95Hz$.

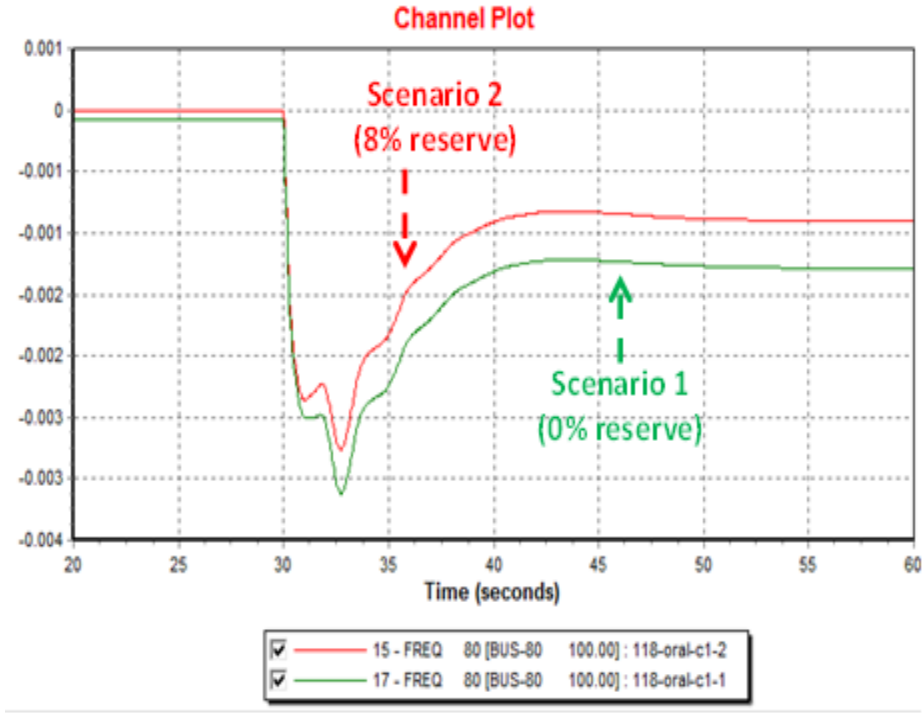


Figure 36 Frequency Responses in Scenario 1 and 2 from 20s-60s

Compared the frequency responses in first 60 seconds in Figure 36, we can observe:

For Stage 1: The rotor swings at bus-80 becomes smaller when there is a spinning reserve in the system. For Stage 3: Since the spinning reserve is 8% in scenario 2, there is a secondary loop control in stage 3.

Given two frequency response figures above, it is easy to conclude that the spinning reserve of a system has a great influence on the frequency deviation. The larger the reserve is, the smaller the frequency deviation will be.

5.2.2.2 Mechanical Power at Bus-80 in Scenario 1 and 2

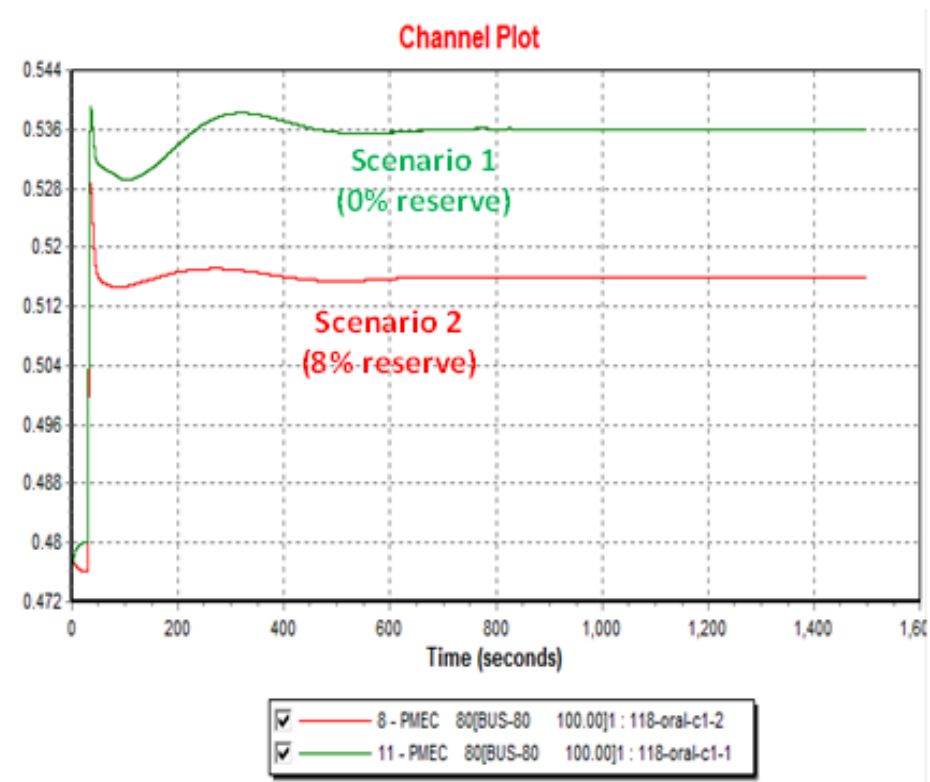


Figure 37 Mechanical Power at Bus-80 in Scenario 1 and 2

Figure 37 clearly shows the importance of spinning reserve to the system. When there is no reserve, in order to gain the balance by droop control, there will be a large frequency

deviation and a big $\Delta P_M = 0.536 - 0.477 = 0.059$ p.u. When there is 8% reserve, there will be a smaller frequency deviation and a smaller $\Delta P_M = 0.516 - 0.477 = 0.039$ p.u. The droop characteristic is shown in Equation (35) below.

$$\Delta P_M = -\frac{1}{R} \Delta \omega \quad (35)$$

5.2.3 Scenario 3 and Scenario 4

5.2.3.1 Scenario 3

Trip 14% output when all the generators are at their maximum output (0% reserve, no secondary loop). The load model consists of 30% constant current and 70% constant impedance.

In this case, all the generators have hit the limits and there is no spinning reserve. Here we just randomly pick bus 10, bus 80 and bus 89 and the results of these three buses are shown below in Table 8.

Table 8 Results Compared in Scenario 3

| Bus No. | PFLTFS | PSS/E |
|-------------------|---------------|--------------|
| 10(volt) | 1.05 | 1.05 |
| 10(output) | 4.59 | 4.45 |
| 80(volt) | 1.04 | 1.03 |
| 80(output) | 4.86 | 5.36 |
| 80(load) | 1.39 | 1.28 |
| 89(volt) | 0.99 | 1.00 |
| 89(output) | 0 | 0 |
| Frequency | 59.87 Hz | 59.92 Hz |

The error between two frequencies is 0.08%.The system settled down at $t = 1008s$ with a new system frequency $f = 59.92$ Hz.

5.2.3.2 Scenario 4

Trip 14% output when all the generators are at their maximum output (0% reserve, no secondary loop). The load model consists of 30% constant current and 70% constant impedance.

In this case, the generators haven't hit the limits and there is 8% spinning reserve. Here we just randomly pick bus 10, bus 80 and bus 89 and the results of these three buses are shown below in Table 9.

Table 9 Results Compared in Scenario 4

| Bus No. | PFLTFS | PSS/E |
|-------------------|---------------|--------------|
| 10(volt) | 1.05 | 1.05 |
| 10(output) | 4.91 | 4.57 |
| 80(volt) | 1.04 | 1.04 |
| 80(output) | 5.20 | 5.17 |
| 80(load) | 1.39 | 1.29 |
| 89(volt) | 0.99 | 1.00 |
| 89(output) | 0 | 0 |
| Frequency | 59.95 Hz | 59.95 Hz |

The error between two frequencies is 0%. The system settled down at $t = 1074s$ with a new system frequency $f = 59.95$ Hz.

5.2.4 Scenario 5

This section will give the results of some severe unbalanced IEEE 118-bus systems. More than 30% of the total generation will be tripped and the droop R and its inverse parameter K will also be modified to see the influence to the system frequency. The system frequency will decrease to 58 Hz level.

In order to simplify the dynamic simulation model, here we just use constant impedance model for loads.

For most cases, we compared the settled down system frequency results from static state method (the PFLTFS method) and the dynamic simulation (PSS/E), settled down time in dynamic simulation are also compared between the cases whose system has some spinning reserve and which has not.

1. Trip 30% of the total generation (Table 10)

Table 10 Frequency Results (30% Output Tripped)

| | PFLTFS (Hz) | PSS/E (Hz) | Error | Settle T (s) |
|-------------------|-------------|------------|-------|--------------|
| 0% reserve | 59.73 | 59.83 | 0.16% | 993 |
| 8% reserve | 59.78 | 59.85 | 0.12% | 1095 |

2. Trip 40% of the total generation (Table 11)

Table 11 Frequency Results (40% Output Tripped)

| | PFLTFS (Hz) | PSS/E (Hz) | Error | Settle T (s) |
|-------------------|--------------------|-------------------|--------------|---------------------|
| 0% reserve | 59.66 | 59.76 | 0.17% | 1050 |
| 8% reserve | 59.69 | 59.78 | 0.15% | 1106 |

3. Trip 50% of the total generation (Table 12)

Table 12 Frequency Results (50% Output Tripped)

| | PFLTFS (Hz) | PSS/E (Hz) | Error |
|-------------------|--------------------|-------------------|--------------|
| 0% reserve | 59.47 | 59.53 | 0.10% |
| 8% reserve | 59.51 | 59.56 | 0.08% |

From case 1 and case 2 it is obvious to see, the system with a spinning reserve will take longer for the system to settle down since the secondary loop control exists and it costs time to moving towards to the maximum reference set point.

For case 3 there is no settled time for dynamic simulation, because this is a very severe situation. The system voltage will collapse if we trip 50% real power output at one time. The tripping units are shut down one by one, so it is not possible to count the settled down time.

4. Trip 40% of the total generation $K = 18$ (Table 13)

Table 13 Frequency Results (40% Output Tripped, K=18)

| | PFLTFS (Hz) | PSS/E (Hz) | Error |
|-------------------|--------------------|-------------------|--------------|
| 0% reserve | 58.95 | 59.75 | 1.3% |
| 8% reserve | 59.07 | 59.77 | 1.1% |

5. Trip 40% of the total generation K = 8 (Table 14)

Table 14 Frequency Results (40% Output Tripped, K=8)

| | PFLTFS (Hz) | PSS/E (Hz) | Error |
|-------------------|--------------------|-------------------|--------------|
| 0% reserve | 57.63 | 58.61 | 1.6% |
| 8% reserve | 57.90 | 58.73 | 1.3% |

In case 4 and case 5 we lower the value of K to make the frequency deviation larger. Compared to case 2 in which the inverse droop characteristic K (1/R) is set to be 50, the smaller the K is, the larger system frequency deviation is and less stable the whole system is.

CHAPTER VI

DISCUSSION AND CONCLUSION

As an extension of some previous studies on power flow method and motivated by the long term frequency stability issues in power system, the work presented here has focused on a novel power flow method which incorporate the frequency deviation as a state variable.

A novel power flow for long term frequency stability method (the PFLTFS method) which can be used to do the power flow calculation for an abnormal system whose real power outputs cannot cover the load demands is proposed here. The method has been applied to a 4-bus system and the IEEE 118-bus system. These power flow solutions are verified by the results from PSS/E dynamic simulation.

The frequency control system and the long term frequency response are introduced in details in this work. The plots from the PSS/E dynamic simulation have helped to track the system frequency behavior after a big units tripping and to analyze the typical long term frequency response.

6.1 Possible Causes of the Frequency Difference

1. In PSS/E, “TGOV1” turbine governor model (only primary loop control) is used for some generators whose output is less than 100 MW. That is to say, only the generators whose output is larger than 100 MW have secondary loop control in the long term dynamic simulation. Although this is close to fact, it is slightly different from the PFLTFS method.

In the novel static state power flow method - PFLTFS, all the generators are considered to have only primary control.

2. In PSS/E, the voltage regulators cannot bring the voltages back to their initial value after tripping units. There exist steady state errors to the voltage setting value in the dynamic simulation that cannot be offset by the voltage regulators. However in PFLTFS, all the regulated voltages are always fixed to their initial value.

The minor difference in voltage will also cause the difference in load and current. Thus it affects whole system power flow solution.

3. As we mentioned above, the load in PSS/E is slightly different from that in PFLTFS, because the load model is tightly related to the voltage.

4. Some minor frequency fluctuations have been neglected might also be a reason for the different system frequency got from dynamic simulation. In PSS/E, “Extended term simulation (MSTRT)” is used to perform the long term dynamic simulation. The higher frequency effects associated with system disturbances have been subsided [28].

6.2 Conclusion

The main conclusions of the thesis are summarized below.

1. With the a much higher penetration of renewable energy in the system, such as wind energy and solar energy, the frequency stability is becoming more vulnerable to sudden generation and demand changes. The mismatch between real power output and load demand problem in the system requires significant effort to ensure the continued reliability of the bulk power system.

2. The PFLTFS method proposed in this thesis incorporate the frequency deviation into the state variables. This method provides a technique for solving an abnormal state system power flow. A 4-bus system and the IEEE 118-bus system are considered as the tests system. From the

results we can conclude that the PFLTFS method is reasonable for solving power flow of a real power unbalanced system.

3. This novel power flow only finds the final state which we care mostly. We bypassed the lengthy dynamic calculations to save computation time and to directly compute the steady state power flow solutions that include line flow information.

To run a 4-bus system dynamic simulation for 30 minutes response, it usually takes 50 seconds. But using the novel power flow, the computation time will reduce to several seconds. For bigger systems such as the IEEE 118-bus system, it takes dynamic simulation 116 seconds to run the frequency response with 14% units tripping. For severe cases, the dynamic simulation will take up to 237 seconds to run the response. However, the PFLTFS method computation time is still within 10 seconds. Note that PSS/E is a commercial software, whose codes have been optimized. On the other hand, we use Matlab, which is rather primitive for feasibility and demonstration purposes. In reality, after code optimization, the speedup will be even more substantial.

Related Laptop CPU Info:

Intel(R) Core(TM)2 Duo CPU P8800 @ 2.66 GHz 2.66 GHz

DDR3 1067MHz 4GB*2 RAM

4. The effect of the droop characteristic in frequency stability studies has been investigated in this thesis. Primary control is the most critical part of frequency control because unlike secondary loop control, the primary control always exists. Thus the primary control has to be ensured to always react properly, and the value of droop should also be set reasonably.

5. If there is a large units tripping (more than 10%) in a system, there will be a long term distortion in power balance. Usually it takes 15 to 20 minutes for the long term frequency response in the system to settle down to a new system frequency and regain the balance state.

6. According to the frequency results in chapter 4, an adequate spinning reserve of power should be remained in the generator. Reactive power reserve can help prevent voltage collapse and real power reserve can reduce frequency deviation. Reserves which can help maintain supply and demand balance are critical during primary and secondary frequency control. [29]

7. When there is a spinning reserve power in the generator, it takes longer (around 50s to 60s) for the system to settle down to a new frequency because the secondary loop control will be involved in frequency response.

8. Frequency deviation is related to both spinning reserve and droop characteristic. The droop characteristic helps offset the system real power mismatch by decreasing the system frequency accuracy. Although the droop control can cover the power balance in the system, it results in the frequency deviating from the nominal frequency.

In addition, due to the droop control, a steep R can minimize the frequency deviation. A steeper droop should be used since it is more useful for the system frequency stability.

REFERENCES

- [1] K. Rave, S. Teske and S. Sawyer, "Global Wind Energy Outlook 2012," *Global Wind Energy Council*, http://www.gwec.net/wp-content/uploads/2012/11/GWEO_2012_lowRes.pdf, 2012.
- [2] Wikipedia, "Solar Power," http://en.wikipedia.org/wiki/Solar_power, 2013.
- [3] S.G. Johansson, "Long-term Voltage Stability in Power Systems-Alleviating the Impact of Generator Current Limiters," *Ph. D. dissertation*, Chalmers University of Technology, Göteborg, Sweden, 1998.
- [4] P. Kundur, "Section 2.2: Classification of Stability," in *Power System Stability and Control: Part I*, 1st edition, McGraw-Hill, ISBN: 0070635153, pp. 35, New York, NY, USA, 1994.
- [5] J. Horne, D. Flynn and T. Littler, "Frequency Stability Issues for Islanded Power Systems," *IEEE PES Power Systems Conference and Exposition (PSCE'04)*, Vol. 1, pp. 299-306, 2004.
- [6] S. Iwamoto and Y. Tamura, "A Load Flow Calculation Method for Ill Conditioned Power Systems," *IEEE Trans. on Power App. and Systems*, Vol. PAS-100, No. 4, pp. 285-292, 1981.
- [7] P. Yan, "A Fast Load Flow Model for a Dispatcher Training Simulator Considering Frequency Deviation Effects," *Electrical Power & Energy Systems*, Vol. 20, No. 3, pp. 177-182, 1998.
- [8] P. Alto, "Power System Dynamics Tutorial," *Electric Power Research Institute*, <http://www.epri.com/abstracts/Pages/ProductAbstract.aspx?ProductId=000000000001016042&Mode=download>, 2009.

[9] A. Oberhofer and P. Meisen, “Energy Storage Technologies and Their Role in Renewable Integration,” *Global Energy Network Institute*, <http://www.ourenergypolicy.org/energy-storage-technologies-their-role-in-renewable-integration/>, 2012.

[10] G. Huang, “Lecture 9: Power System Control and Operation: AGC,” in Lecture Slides from *ELEN 615 Power System Stability Analysis Class*, Texas A&M University, pp. 9, College Station, TX, USA, 2011.

[11] J. Machowski, J. W. Bialek and J. R. Bumby, “Section 2.3.3.6: Turbine Characteristics,” in *Power System Dynamics: Stability and Control*, 2nd edition, John Wiley & Sons, ISBN: 9781119965053, pp. 32-34, New York, NY, USA, 2008.

[12] J. Machowski, J. W. Bialek and J. R. Bumby, “Section 9.1.2: Primary Control,” in *Power System Dynamics: Stability and Control*, 2nd edition, John Wiley & Sons, ISBN: 9781119965053, pp. 339-341, New York, NY, USA, 2008.

[13] J. Machowski, J. W. Bialek and J. R. Bumby, “Section 8.5.1: The Dynamics of Voltage Collapse,” in *Power System Dynamics: Stability and Control*, 2nd edition, John Wiley & Sons, ISBN: 9781119965053, pp. 321-323, New York, NY, USA, 2008.

[14] Siemens Inc., “PSS/E Product Information,” *Siemens Corporation*, <http://www.energy.siemens.com/us/en/services/power-transmission-distribution/power-technologies-international/software-solutions/pss-e.htm>, 2013.

[15] Power Technology Inc., “Section 7.10: Extended Term Simulation,” in *PSS/E: Program Operation Manual*, Vol. 1, PTI Inc., pp. 7.43-7.45, Schenectady, NY, USA, 2004.

[16] V. Krish, “Power System Simulation for Engineers: Stability Analysis,” *PTI Inc.*, <https://www.google.com.hk/url?sa=t&rct=j&q=&esrc=s&source=web&cd=3&cad=rja&ved=0CEIQFjAC&url=http%3A%2F%2Fwww.ee.iastate.edu%2F~jdm%2FEE456%2FpsseIntroInstructio>

ns.doc&ei=zIVuUabEKTz2QXFqoDYDw&usg=AFQjCNHqtkbapJMZPSwMAo00ncIYEct3Kg
&sig2=QhCUsvC8cKp4qqd8yZ-91g, 2013.

[17] Siemens Inc., “Section 13.2.4: Equipment Model Selection,” in *PSS/E: Program Application Guide*, Vol. 2, PTI Inc., pp. 13.8, Schenectady, NY, USA, 2010.

[18] Siemens Inc., “Section 13.2.5: Round Rotor Generator Model (Quadratic Saturation) Figure 13-5,” in *PSS/E: Program Application Guide*, Vol. 2, PTI Inc., pp. 13.9, Schenectady, NY, USA, 2010.

[19] Power Technology Inc., “Section 26.5: TGOV5,” in *PSS/E: Program Application Guide*, Vol. 2, PTI Inc., pp. 26.15-26.20, Schenectady, NY, USA, 2010.

[20] Power Technology Inc., “Appendix H: TGOV5,” in *PSS/E: Program Operation Manual*, Vol. 2, PTI Inc., pp. H.41-H.43, Schenectady, NY, USA, 2004.

[21] Siemens Inc., “Section 16.5.5: Model SEXS and REXSYS,” in *PSS/E: Program Application Guide*, Vol. 2, PTI Inc., pp. 16.21, Schenectady, NY, USA, 2010.

[22] Power Technology Inc., “Appendix G: SCRX,” in *PSS/E: Program Operation Manual*, Vol. 2, PTI Inc., pp. G.87, Schenectady, NY, USA, 2004.

[23] Siemens Inc., “Section 16.5.6: Model SEXS,” in *PSS/E: Program Application Guide*, Vol. 2, PTI Inc., pp. 16.21, Schenectady, NY, USA, 2010.

[24] Power Technology Inc., “Appendix G: IEEEET2,” in *PSS/E: Program Operation Manual*, Vol. 2, PTI Inc., pp. G.63-G.64, Schenectady, NY, USA, 2004.

[25] Siemens Inc., “Section 24.2.3: Use of Typical Machine Data: Figure 24-10,” in *PSS/E: Program Application Guide*, Vol. 2, PTI Inc., pp. 24.12, Schenectady, NY, USA, 2010.

[26] Siemens Inc., “Section 16.7.2: Model IEEEEST,” in *PSS/E: Program Application Guide*, Vol. 2, PTI Inc., pp. 16.32-16.33, Schenectady, NY, USA, 2010.

[27] J. Machowski, J. W. Bialek and J. R. Bumby, “Section 9.2: Stage I - Rotor Swings in the Generators,” in *Power System Dynamics: Stability and Control*, 2nd edition, John Wiley & Sons, ISBN: 9781119965053, pp. 350-352, New York, NY, USA, 2008.

[28] G. Andersson, “Dynamics and Control of Electric Power Systems,” *EEH Power Lab*, http://www.eeh.ee.ethz.ch/fileadmin/user_upload/eeh/studies/courses/power_system_dynamics_and_control/Documents/DynamicsPartI_lecture_notes_2012.pdf, 2012.

[29] J. Machowski, J. W. Bialek and J. R. Bumby, “Section 8.5.1.2: Scenario 2: Network Outages,” in *Power System Dynamics: Stability and Control*, 2nd edition, John Wiley & Sons, ISBN: 9781119965053, pp. 321-322, New York, NY, USA, 2008.